NASA TECHNICAL NOTE

NASA TN D-7816

NASA TN D-7816

(NASA-TN-D-7816) STATIC TESTS OF A SIMULATED UPPER SURFACE BLOWN JET-FLAP CONFIGURATION UTILIZING A FULL-SIZE TURBOFAN ENGINE (NASA) 41 p HC $3.75 CSCL 01A

N75-16504

Unclas

H1/01 10669

STATIC TESTS OF A SIMULATED UPPER SURFACE BLOWN JET-FLAP CONFIGURATION UTILIZING A FULL-SIZE TURBOFAN ENGINE

James P. Shivers and Charles C. Smith, Jr.

Langley Research Center
Hampton, Va. 23665

MAR 1975 RECEIVED

NATIONAL AERONAUTICS AND SPACE ADMINISTRATION • WASHINGTON, D. C. • FEBRUARY 1975

1. Report No.	2. Government Accession No.	3. Recipient's Catalog No.
NASA TN D-7816		

4. Title and Subtitle	5. Report Date
STATIC TESTS OF A SIMULATED UPPER SURFACE BLOWN JET-FLAP CONFIGURATION UTILIZING A FULL-SIZE TURBOFAN ENGINE	February 1975
	6. Performing Organization Code
7. Author(s)	8. Performing Organization Report No.
James P. Shivers and Charles C. Smith, Jr.	L-9712
	10. Work Unit No.
9. Performing Organization Name and Address	760-61-02-01
NASA Langley Research Center Hampton, Va. 23665	11. Contract or Grant No.
	13. Type of Report and Period Covered
12. Sponsoring Agency Name and Address	Technical Note
National Aeronautics and Space Administration Washington, D.C. 20546	14. Sponsoring Agency Code

15. Supplementary Notes

16. Abstract

The investigation utilizing a small turbofan engine was conducted to evaluate static turning performance and pressure and temperature environment of an upper surface blown wing and flap segment. The tests involved modifications of the engine primary nozzle to alleviate high-temperature problems on the wing and flaps without adversely affecting static turning performance over the desired range of flap deflection and thrust condition.

17. Key Words (Suggested by Author(s))	18. Distribution Statement
Aerodynamics Powered lift Upper surface blown jet flap Fluid mechanics	Unclassified – Unlimited STAR Category 01

19. Security Classif. (of this report)	20. Security Classif. (of this page)	21. No. of Pages	22. Price*
Unclassified	Unclassified	39	$3.75

*For sale by the National Technical Information Service, Springfield, Virginia 22151

STATIC TESTS OF A SIMULATED UPPER SURFACE BLOWN JET-FLAP CONFIGURATION UTILIZING A FULL-SIZE TURBOFAN ENGINE

James P. Shivers and Charles C. Smith, Jr.
Langley Research Center

SUMMARY

An investigation utilizing a small (9786-N (2200-lb) thrust) turbofan engine has been conducted to evaluate static turning performance and pressure and temperature environment of an upper surface blown (USB) wing and flap. The static-test configuration employed the propulsion system and the wing and flap design of a large USB wind-tunnel model. The exhaust (secondary) nozzle was a fixed design intended to provide attached flow on the upper surface of the wing-flap system. This rectangular nozzle had an aspect ratio (width/height) of 6.0. Results were obtained for several modifications of the hot-core (primary) nozzle and for a range of flap deflection and thrust condition. An acceptable compromise between static turning performance and surface-temperature constraints was obtained with an elliptical primary nozzle which replaced the original round primary nozzle. Measurements of flow characteristics over the wing and flap surfaces indicated attached flow even at the largest flap deflection and revealed a very rapid decay of peak velocities from the exhaust-nozzle exit to the flap trailing edge.

INTRODUCTION

As part of a general research program to provide fundamental information on the upper surface blown (USB) jet-flap concept, the present investigation, utilizing a small (9786-N (2200-lb) thrust) turbofan engine, was conducted to evaluate static turning performance as well as pressure and temperature environment on a USB wing and flap. The apparatus used in this investigation was an outdoor static test stand supporting a JT15D-1 turbofan engine which was equipped with a canted rectangular nozzle with an aspect ratio of 6.0. The engine and nozzle were oriented to direct the jet efflux on to the upper surface of a boilerplate wing-flap system. The test configuration was an adaptation of the propulsion system and wing-flap design of the twin-engine USB wind-tunnel model shown in figure 1. This large-scale model was equipped with two JT15D-1 engines. The wing had double-slotted trailing-edge flaps. Directly behind the engine, the trailing-edge flaps were covered with a metal plate representing a Coanda flap.

The primary objective of this investigation was to establish a configuration that would provide acceptable static turning performance over the desired range of flap-deflection angle without exceeding temperature constraints on wing and flaps. Since the temperature environment on the upper surface of the wing and flap of the wind-tunnel model was a prime consideration, this investigation involved modifications of the primary, or core, nozzle to alleviate high-temperature problems on the wing and flap upper surfaces. This investigation also included surface pressure measurements on the wing and flaps aft of the rectangular nozzle which provide indications of attached flow and are otherwise useful for estimating loads.

SYMBOLS

Measurements were made in U.S. Customary Units. They are presented herein in the International System of Units (SI) with the equivalent values in U.S. Customary Units given parenthetically.

F_A axial force, N (lb)

F_N normal force, N (lb)

F_R resultant force, $\sqrt{F_N^2 + F_A^2}$, N (lb)

h vertical dimension of the aspect-ratio-6.0 secondary exhaust nozzle, cm (in.)

ℓ length of wing surface aft of nozzle, cm (in.)

r radius of Coanda flap surface, cm (in.)

T static thrust, N (lb)

T_1 temperature measurement at the thermocouple nearest wing surface, K (^oF)

T_2 temperature measurement at the thermocouple farthest from wing surface, K (^oF)

x horizontal projected dimension of Coanda flap, cm (in.)

δ_f deflection of Coanda flap upper surface at flap trailing edge relative to wing-chord plane, deg (see table I)

δ_{f2} deflection angle of second element of double-slotted flap of the wind-tunnel model with respect to the wing-chord plane, deg (see table I)

δ_j jet-deflection angle relative to wing-chord plane, deg

η flap-system turning efficiency, F_R/T

Abbreviation:

rpm revolutions per minute

MODEL AND APPARATUS

General Arrangement

The outdoor static-test apparatus is illustrated in figure 2. The engine used in this series of tests was the United Aircraft of Canada JT15D-1 turbofan rated at 9786 N (2200 lb) of static thrust at sea-level standard conditions. This engine has a bypass ratio of 3.34 and a fan pressure ratio of 1.53. The simulated wing and flap system was of boilerplate fabrication with the surface contours similar to those of the airplane shown in figure 1. Details and dimensions of the static-test apparatus are given in figure 3. The entire model including inlet, engine, exhaust nozzles, and wing-flap structure was mounted on a floating frame instrumented to measure both normal and axial forces relative to the engine center line. Three parts of the model were mounted to the floating frame independently: (1) the inlet was rigidly mounted to the engine support truss, (2) the engine was mounted on thrust beams (at the forward engine-mount pivots) which were in turn mounted to the engine support truss, and (3) the wing-flap structure was directly mounted to the floating frame. A rubber seal joined the inlet to the engine fan case, and the secondary-nozzle exit was positioned so that it did not contact the wing-flap structure. This arrangement permitted direct measurement of thrust loads of the engine-nozzle combination independent of the normal and axial loads determined from the floating-frame strain gages. Although tests were conducted with two different inlets (the airplane inlet shown in fig. 2 and the bellmouth inlet shown in fig. 3), there was no discernible effect of inlet configuration on the static-thrust calibrations.

Exhaust-Nozzle Arrangement

The secondary nozzle was a fixed design intended to provide attached flow on the upper surface of the wing-flap system. The rectangular secondary-nozzle exit had an aspect ratio (width/height) of 6.0 and was canted to provide thrust inclination on to the

wing upper surface (about 12° to the wing-chord plane). The basic primary nozzle was mounted inside the secondary nozzle with its circular exit about 1.0 fan diameter upstream of the secondary-nozzle exit. During the course of the investigation, the primary nozzle was modified as shown in figure 4. One modification was a simple half-frustum deflector added to the basic round primary nozzle. (See fig. 4(b).) Another modification was the elliptical-exit primary nozzle illustrated in figure 4(c) which had the same exit area as the basic round nozzle.

Wing and Flaps

The wing and flap as shown in figures 2 and 3 were of boilerplate construction, the wing surface representing the equivalent surface for the wind-tunnel model. The simulated wing on the test stand was mounted with the chord line set at an incidence angle of 0° relative to the engine-nacelle center line.

The Coanda flaps were designed to be interchangeable on the wing. These flaps were essentially curved plates configured to fit tangentially the upper surface contours of the double-slotted flap system for the wind-tunnel model. The four test Coanda flap settings, therefore, are related to four selected deflection angles of the double-slotted flaps (flaps nested and $\delta_{f2} = 20°$, 40°, and 60°). The geometric characteristics of the wing and flaps as related to the secondary nozzle and to the wing-chord plane are presented in table I. In this investigation the significant flap-deflection parameter is the tangency angle at the Coanda flap trailing edge which is defined as δ_f. (See sketch in table I.)

Surface Pressure and Temperature Instrumentation

The wing and flaps were fitted with surface pressure ports and also with surface thermocouples. Locations of the pressure ports are given in figure 5, and locations of the thermocouples are given in figure 6. The pressure ports were connected to a multitube manometer. The thermocouples were connected to a multichannel temperature recorder.

TESTS AND PROCEDURES

First, tests were conducted with the wing and flap removed from the stand to calibrate the engine thrust with the aspect-ratio-6.0 secondary nozzle installed. Although the JT15D-1 engine is rated at 9786 N (2200 lb) of static thrust at sea-level standard conditions, maximum thrust in this series of tests was limited to 8896 N (2000 lb) to avoid gas-turbine overtemperature problems resulting from the use of nonoptimized nozzles. A pitot static rake was mounted vertically across the center line of the exhaust,

and the engine was operated at different power settings to calibrate thrust as a function of engine speed. After the engine thrust was calibrated, the wing and flap were installed and additional tests were made for the range of flap-deflection angle given in table I. Forces measured from the strain gages, pressure distributions measured from the manometer, and temperatures measured from the thermocouples were recorded simultaneously. A photograph was made of the manometer board that registered pressure distributions across the secondary nozzle and over the wing and flap.

RESULTS AND DISCUSSION

The results of this investigation are presented in terms of static turning performance, pressure distributions on the wing and flaps, velocity distribution from the secondary nozzle, velocity profiles of flow over the wing and flaps, and temperature measurements on the wing and flap surfaces and in the gas flow from the nozzle exit. The primary variables were flap-deflection angle, hot-nozzle modifications, and thrust level. Emphasis has been placed on the extreme condition of maximum thrust (approximately 8896 N (2000 lb)) in the presentation of data.

Exhaust-Nozzle Flow Characteristics

Characteristics of the efflux at the exit plane of the secondary nozzle were first evaluated with the wing and flap removed. Velocity profiles across the secondary-nozzle exit with the round primary nozzle (at an engine thrust of 8896 N (2000 lb)) and with the elliptical primary nozzle (at an engine thrust of 7784 N (1750 lb)) are compared in figure 7. (The elliptical nozzle was tested after the round nozzle. At this time an operational procedure had been established to run the engine at reduced thrust to minimize chance of damage to the engine, since there was no spare engine.) A high-velocity region around the middle of the secondary nozzle is apparent with the round primary nozzle (fig. 7(a)). This high-velocity region was spread laterally by the elliptical primary nozzle (fig. 7(b)). Also, the elliptical primary nozzle introduced some distortions in the velocity profiles which are probably related to a slight misalinement of the major ellipse axis with respect to the secondary-nozzle axis. Similar velocity-profile data are not available for the round primary nozzle with the deflector.

A comparison of temperature patterns of flow at the secondary-nozzle exit plane with the round primary nozzle and with the elliptical primary nozzle is presented in figure 8. Temperatures were measured at two heights above the location at which the wing upper surface was to be positioned: 4.28 cm (1.685 in.) and 11.58 cm (4.560 in.). With the round primary nozzle, peak temperatures of the order of 811 K (1000° F) occurred along the center line and were not greatly different at the two vertical heights (fig. 8(a)). With the elliptical primary nozzle, there was considerable spanwise distortion of the

temperature patterns at the two vertical heights, and the peak temperatures of the order of 644 K (700° F) did not necessarily occur on the nozzle center line (fig. 8(b)). This distortion of the temperature pattern with the elliptical primary nozzle is probably related to the previously mentioned misalinement of the major ellipse axis relative to the secondary-nozzle axis. The main point of these results is the general lowering of peak temperatures from the order of 811 K (1000° F) to the order of 644 K (700° F) by changing from a round primary nozzle to an elliptical primary nozzle.

Temperature data were obtained only at the secondary-nozzle center line for the round primary nozzle equipped with the deflector, and in figure 9 these results are compared with similar data for the basic round primary nozzle. Temperatures at the two vertical heights were essentially equal and of the order of 811 K (1000° F) with the basic round primary nozzle (fig. 9(a)). With the deflector on the round nozzle, the temperature at the measuring points nearest the wing surface location dropped to about 511 K (460° F), whereas the temperatures at the measuring point away from the wing surface location increased to about 866 K (1100° F) (fig. 9(b)). Use of the deflector on the primary nozzle should therefore be effective in reducing temperatures on the wing surface.

Static Turning Characteristics

The effectiveness of an upper surface blown jet flap in forward flight is dependent to a large degree on how well the engine efflux attaches to the deflected upper surface of the wing and flap and on the efficiency of turning the jet sheet, and consequently the thrust vector. Static turning tests were made, therefore, to determine these characteristics as functions of the engine primary-nozzle geometry, trailing-edge flap-deflection angle, and engine-thrust level. For each test configuration, the engine static thrust was determined as a function of fan speed with the wing surface and flap removed. The engine static thrust for the configuration with the basic round primary nozzle was the same as the static thrust for the configuration with the elliptical primary nozzle. When the deflector was added to the round nozzle, there was a slight loss in static thrust as can be seen in figure 10. Although some of these tests were conducted with a nacelle inlet designed for the large-scale wind-tunnel model and others were conducted with a bellmouth inlet, there was no discernible effect of inlet configuration on the static-thrust calibrations.

The results of the static turning tests are presented in figure 11. The static turning performance is presented in terms of the jet-deflection angle δ_j and the flap turning efficiency η (which is a measure of the static-thrust recovery at the jet-deflection angle achieved). Both the flap-deflection angle δ_f and the jet-deflection angle δ_j are referenced to the wing-chord plane which was parallel with the engine center line. The flap-deflection angle δ_f is defined as the deflection of the upper surface tangency line at the flap trailing edge with respect to the wing-chord plane. Thus, for the clean con-

figuration, corresponding to the upper surface of the basic airfoil, the upper surface tangency angle δ_f was 9.2°. The aspect-ratio-6.0 secondary nozzle was configured to direct the jet sheet on to the upper surface of the wing at an angle of 11.75° with respect to the engine center line. This thrust-axis inclination was confirmed experimentally during engine thrust calibrations with the wing and flap removed. (See fig. 11(a).)

Effect of primary-nozzle geometry.- Static turning tests were originally conducted with a standard primary nozzle having a round exit. As shown in figure 11(a), tests conducted with this round primary nozzle at the $\delta_f = 70°$ configuration provided fairly good static turning performance at a very high efficiency $(\delta_j = 58°$ and $\eta = 0.97)$. This round primary nozzle, however, caused a high-temperature problem on the wing upper surface and on the knee of the Coanda flap because of direct impingement by the hot-core flow. Therefore, the primary nozzle had to be modified to relieve this temperature problem. Tests were conducted with a deflector on the primary-nozzle exit which diverted the hot-core flow off the wing surface. (See fig. 4.) As shown in figure 11(a), when this deflector was used on the round primary nozzle at the same flap-deflection angle ($\delta_f = 70°$), the static turning performance suffered appreciably $(\delta_j = 51°$ and $\eta = 0.83)$. This loss in jet-deflection angle and flap turning efficiency is attributed to turbulence created by the deflector and to reduction of impingement angle on to the wing surface. The engine was then fitted with a modified primary nozzle having an elliptical exit as illustrated in figure 4. This nozzle was designed to spread the hot-core flow inside the aspect-ratio-6.0 secondary nozzle for the purpose of relieving the temperature problem without actually diverting the hot-core flow off the wing surface. As shown in figure 11(a), static turning tests conducted with the elliptical primary nozzle at the same flap-deflection angle ($\delta_f = 70°$) provided static turning performance much better than that obtained with the deflector on the round nozzle and almost as good as that obtained with the original round primary nozzle $(\delta_j = 55°$ and $\eta = 0.93)$. As is shown in a subsequent section, this elliptical primary nozzle also provided the required temperature relief on the upper surface of the wing and flap.

Effect of trailing-edge flap deflection.- Static turning tests were conducted over the range of flap deflection only for the configuration with the deflector on the round primary nozzle. These results shown in figure 11(b) indicate reasonably good static turning performance for all flap deflections except $\delta_f = 70°$ (turning angle losses ranged from 2° to 8° and η was greater than 0.90). By inference, static turning performance with the elliptical primary nozzle should at least equal that obtained with the deflector on the primary nozzle over the lower range of flap deflection.

Effect of thrust level.- The static turning performance as a function of thrust level for $\delta_f = 70°$ is presented in figure 11(c) for the elliptical primary nozzle and for the round primary nozzle with the deflector. The static turning performance for the ellipti-

cal nozzle was reasonably good over the test range of thrust ($\delta_j \approx 55^o$ and $\eta \approx 0.93$). The results also indicate considerably less dispersion of data over the thrust range with the elliptical nozzle than with the round nozzle with the deflector.

Flow Characteristics With Wing and Flaps Installed

During the tests to determine the static turning characteristics, measurements were also made of surface pressures and temperatures on the wing and flaps and of flow velocities and temperatures in the region above the wing-flap surface. As mentioned previously, the objective of this investigation was to determine an acceptable compromise between static turning performance and surface-temperature constraints on the wing and flaps. The following sections describe the wing-flap environment as a function of modifications of the primary nozzle.

Surface pressures and temperatures.- The results of surface-pressure measurements on the wing and flaps aft of the aspect-ratio-6.0 secondary nozzle are presented in figures 12 and 13, and the results of corresponding surface-temperature measurements are presented in figures 14 to 16.

Shown in figure 12 are surface-pressure data with the round primary nozzle and at 70^o flap deflection, and corresponding surface-temperature data are shown in figure 14. The pressure data are presented as chordwise pressure profiles with leaders directed from each pressure port. Arrowheads on the leaders indicate pressure direction (down for positive pressure on the surface and up for negative or suction pressure on the surface), and the length of the leaders reflects the magnitude of individual pressures. The results shown in figure 12 provide a good indication of attached flow well back toward the trailing edge. Also, suction pressures are generated forward of the flap on the wing surface except on the center line where positive pressures occurred because of jet impingement. The high-temperature problem on the wing and flap surface (fig. 14) is associated with impingement of hot primary flow from the round nozzle. Temperatures of the order of 700 K (800^o F) were measured just forward of the flap.

To relieve the surface-temperature problem, the deflector shown in figure 4 was installed on the round primary nozzle. Surface-pressure data obtained with this modification are presented in figure 13, and corresponding surface-temperature data are presented in figure 15 through the test range of flap deflection. The data of figures 13(d) and 15(d) are for flap deflection of 70^o and may, therefore, be directly compared with the previously discussed results for the basic round primary nozzle. The deflector on the primary nozzle turned the hot-core flow away from the wing surface, so that maximum surface temperatures, which were under 478 K (400^o F), were significantly reduced from those obtained with the basic round primary nozzle. (Compare figs. 14 and 15(d).) The corresponding surface-pressure data of figure 13(d) obtained with the deflector on the

primary nozzle are not appreciably different from those obtained with the basic round primary nozzle (fig. 12).

As pointed out in the section on static turning characteristics, use of the deflector on the primary nozzle resulted in unacceptable turning losses; therefore, the primary nozzle was modified to the elliptical exit shown in figure 4 in order to spread the hot-core flow laterally inside the aspect-ratio-6.0 secondary nozzle. Surface temperatures obtained with this elliptical primary nozzle and for the 70° flap deflection are presented in figure 16 which indicates maximum temperatures just forward of the flap of the order of 533 K (500° F), or about 167 K (300° F) lower than with the basic round nozzle. These 533 K (500° F) surface temperatures were deemed to be acceptable for the stainless-steel skin with a thermal-insulation blanket utilized on the wind-tunnel model. This factor in conjunction with the acceptable static-turning performance caused the elliptical primary nozzle to be selected for the wind-tunnel model.

Flow characteristics above the wing and flaps.- Sample results of the gas-temperature profiles along the nozzle center line in the flow region above the wing and flap are presented in figure 17. Corresponding velocity profiles are presented in figure 18. These data were obtained with the round primary nozzle and with $\delta_f = 70°$ at 8896 N (2000 lb) of thrust. In general, the gas temperatures above the flap surface are considerably lower than the corresponding surface temperatures. This condition indicates that the hot-core flow tends to adhere to the flap surface. The velocity profiles (fig. 18) indicate a rather rapid decay in average velocity as the flow progresses toward the flap trailing edge and a dissipation of energy as the exhaust flow mixes with entrained ambient air. The most important point is that peak velocities of the order of 427 m/sec (1400 ft/sec) at the secondary-nozzle exit decayed to about 152 m/sec (500 ft/sec) at the flap trailing edge. This rapid decay of pead velocity is probably related to rapid mixing of the engine efflux with ambient air as evidenced by the attendant decay in temperature.

SUMMARY OF RESULTS

An investigation utilizing a propulsion system with a full-scale turbofan engine was conducted to establish the static turning performance and flow environmental factors of a specifically designed upper-surface blown jet-flap configuration. The following results were obtained from tests on three primary nozzles inside a rectangular aspect-ratio-6.0 secondary nozzle:

1. Acceptable surface-temperature conditions on the wing and flap were obtained with either an elliptical primary nozzle or a round primary nozzle fitted with a deflector

to divert the hot-core flow away from the wing surface, but unacceptable surface temperatures occurred on the wing with the basic round primary nozzle.

2. The engine static thrust for the configuration with the round primary nozzle was the same as the static thrust for the configuration with the elliptical primary nozzle. When the deflector was added to the round nozzle, there was a slight loss in static thrust.

3. Acceptable static turning performance was obtained with either a circular or an elliptical primary nozzle, but unacceptable static turning performance resulted at the 70° flap-deflection angle when a deflector was used on the round primary nozzle.

4. For the maximum thrust condition and at the largest test flap-deflection angle, peak velocities of the order of 427 m/sec (1400 ft/sec) at the secondary-nozzle exit decayed to about 152 m/sec (500 ft/sec) at the flap trailing edge.

Thus, modification of the round primary nozzle to an elliptical primary nozzle resulted in acceptable surface temperatures without adversely affecting static turning performance or static thrust. Therefore, the elliptical nozzle was selected for the full-scale configuration.

Langley Research Center,
National Aeronautics and Space Administration,
Hampton, Va., January 14, 1975.

TABLE I.- GEOMETRIC CHARACTERISTICS OF WING AND FLAPS

[δ_{f2} refers to the nominal deflection with respect to the wing-chord plane of the second chordwise element of a double-slotted flap]

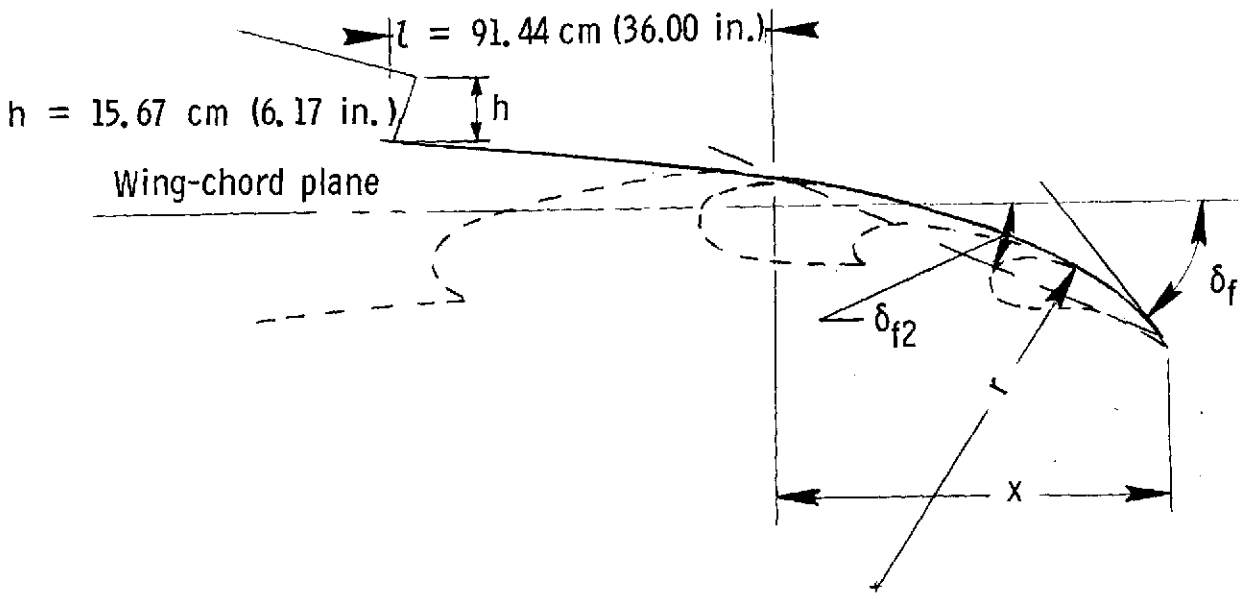

Flap configuration	δ_f, deg	r, cm (in.)	x, cm (in.)
Retracted	9.2		56.52 (22.25)
Extended, $\delta_{f2} = 20^o$	29.8	124.46 (49.00)	99.06 (39.00)
Extended, $\delta_{f2} = 40^o$	50.8	92.08 (36.25)	93.47 (36.80)
Extended, $\delta_{f2} = 60^o$	70.0	79.38 (31.25)	79.25 (31.20)

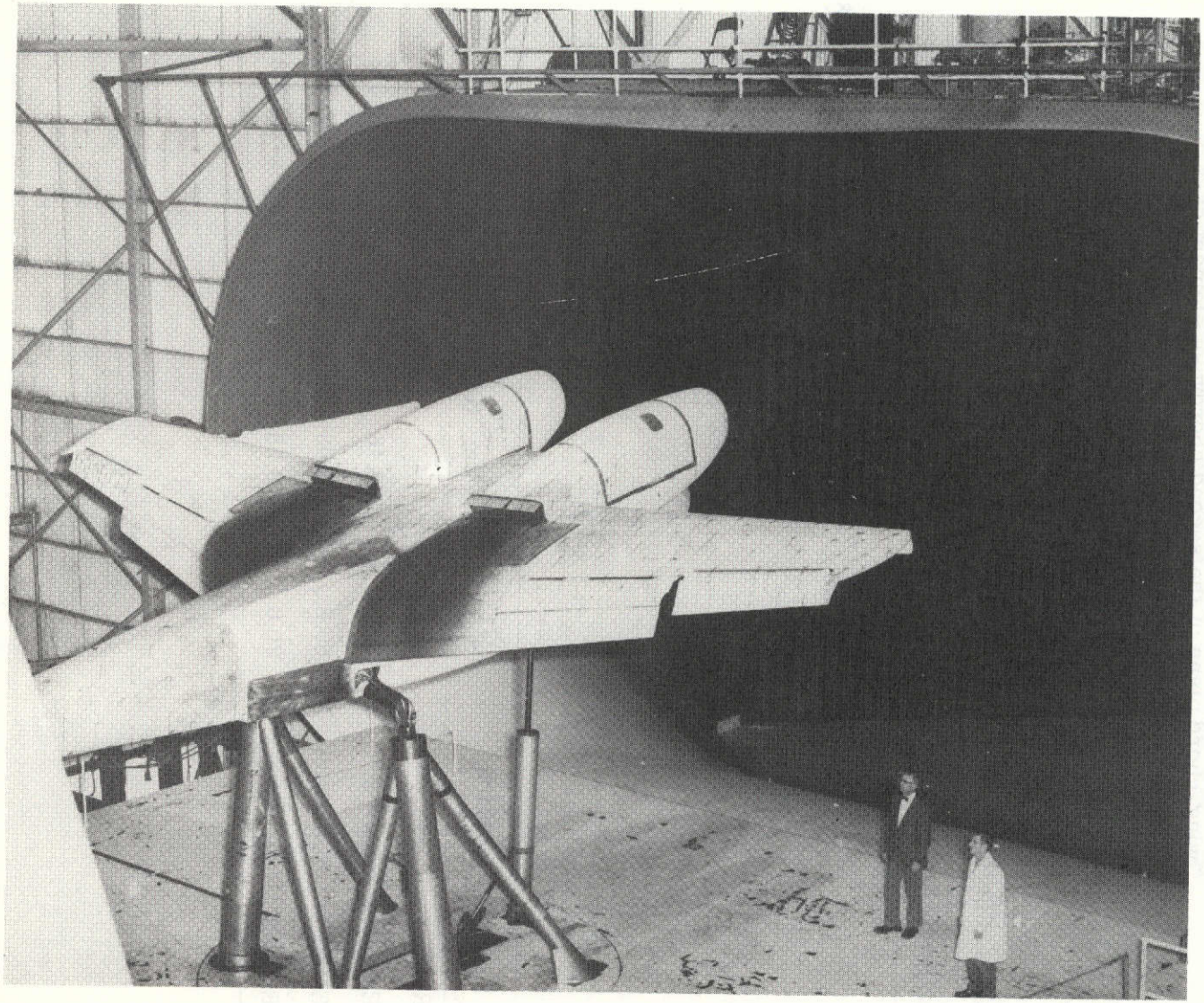

L-74-3231

Figure 1.- Large-scale upper surface blown model mounted in the Langley full-scale tunnel.

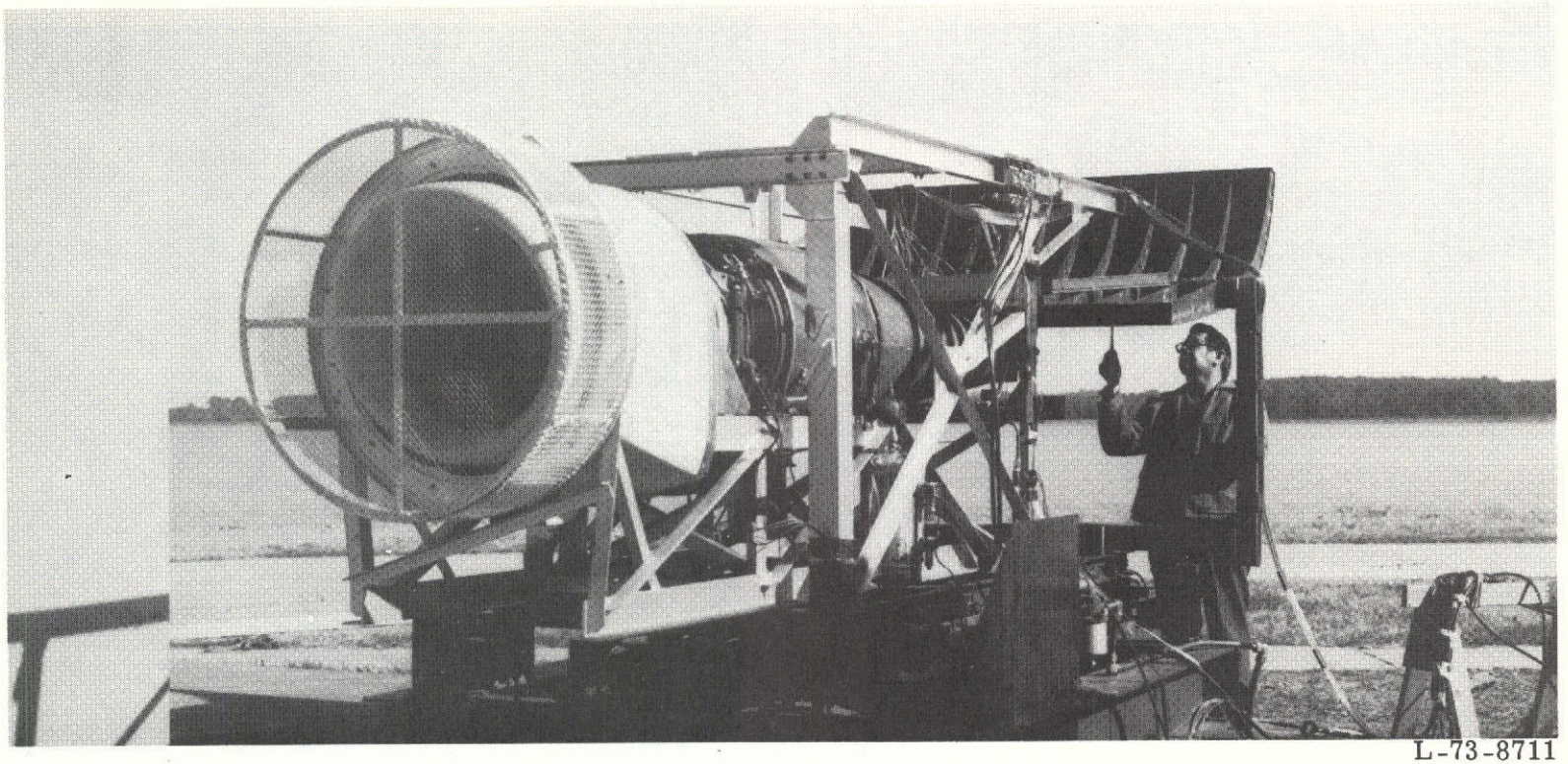

(a) Three-quarter front view.

Figure 2.- Outdoor static-test apparatus with airplane inlet, JT15D-1 turbofan engine, aspect-ratio-6.0 secondary nozzle, and simulated upper surface blown wing and flap.

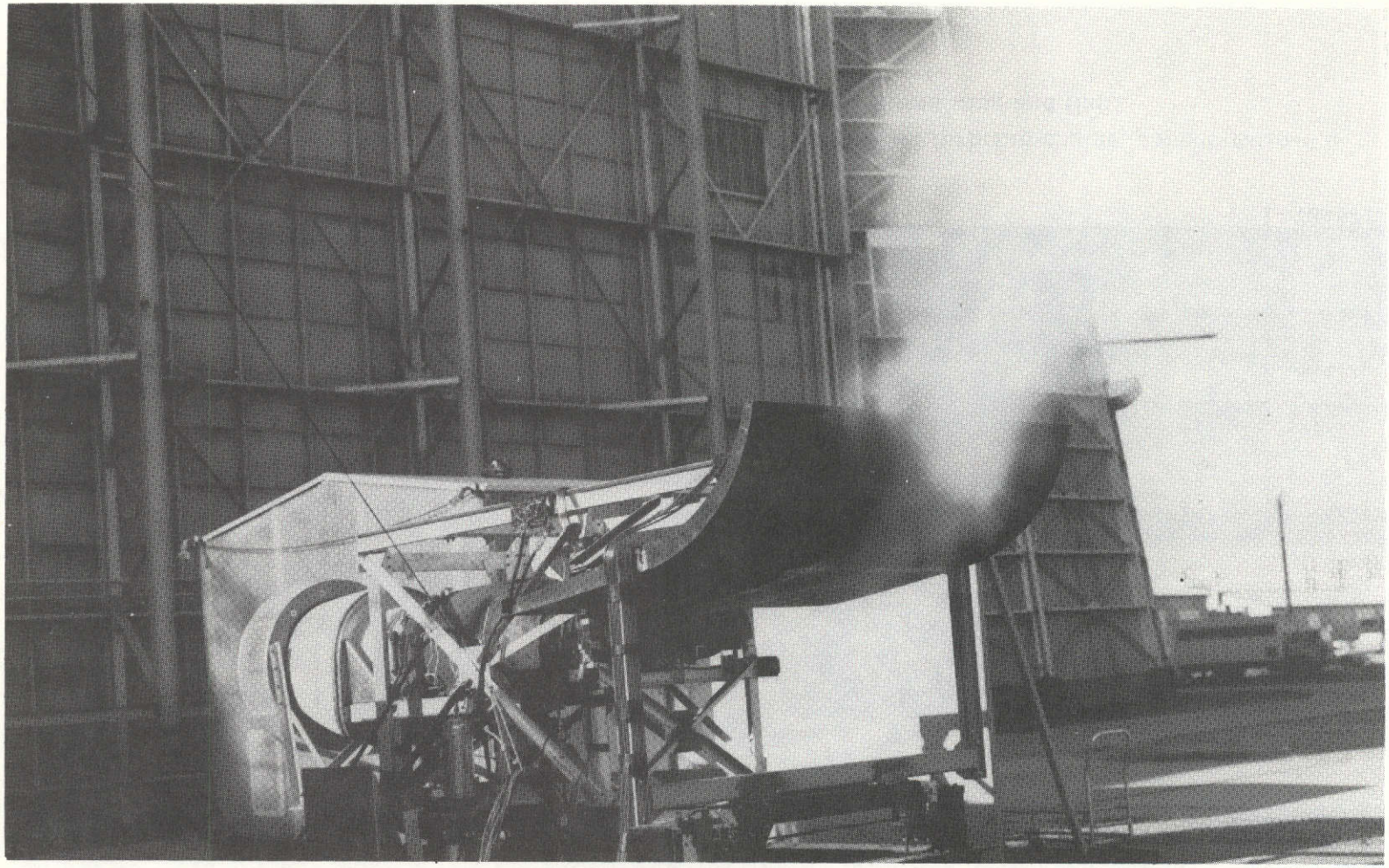

L-73-8709

(b) Three-quarter rear view with smoke to show turning flow.

Figure 2.- Concluded.

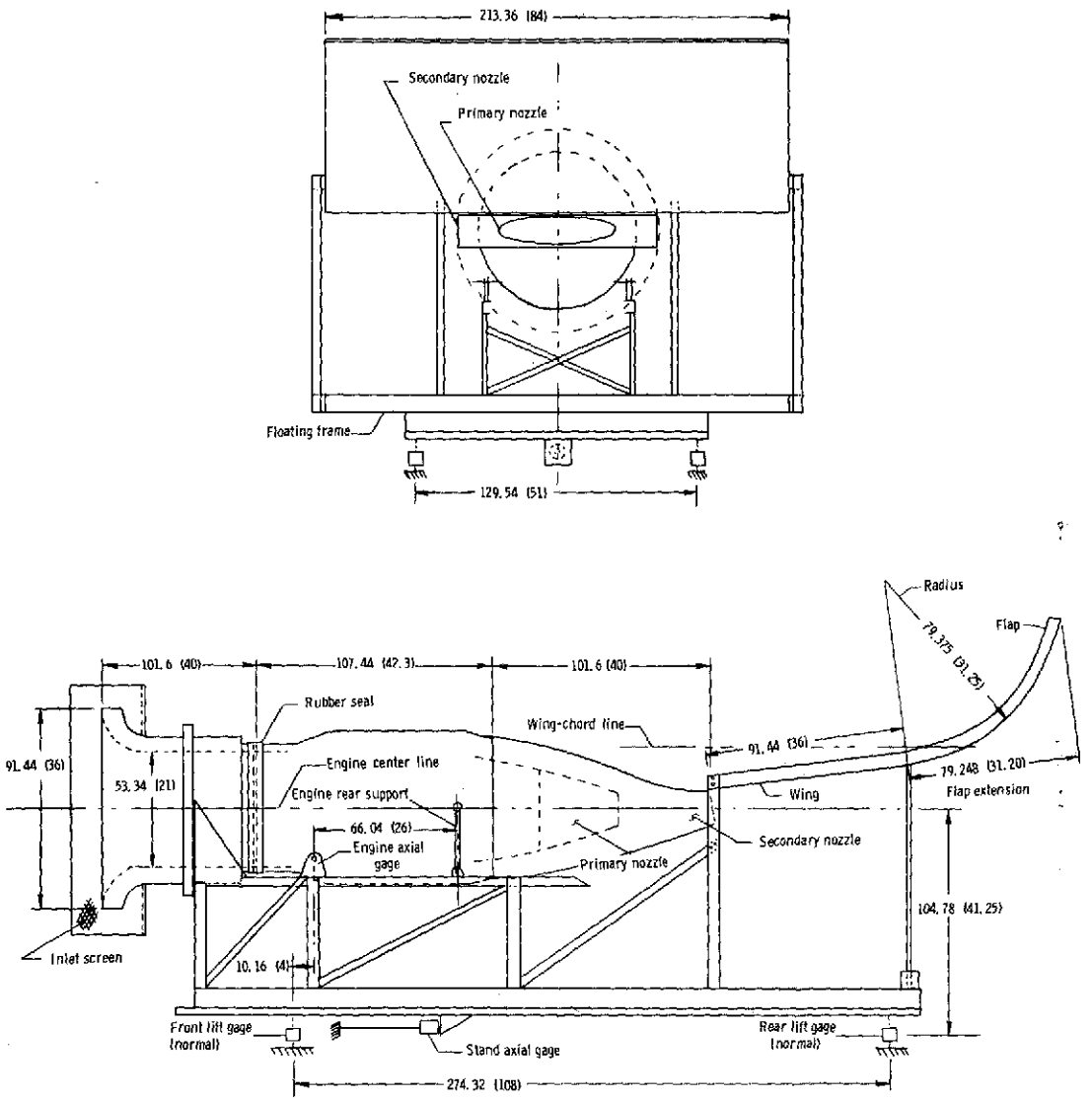

Figure 3.- Sketch of static-test apparatus. Dimensions are in centimeters (inches).

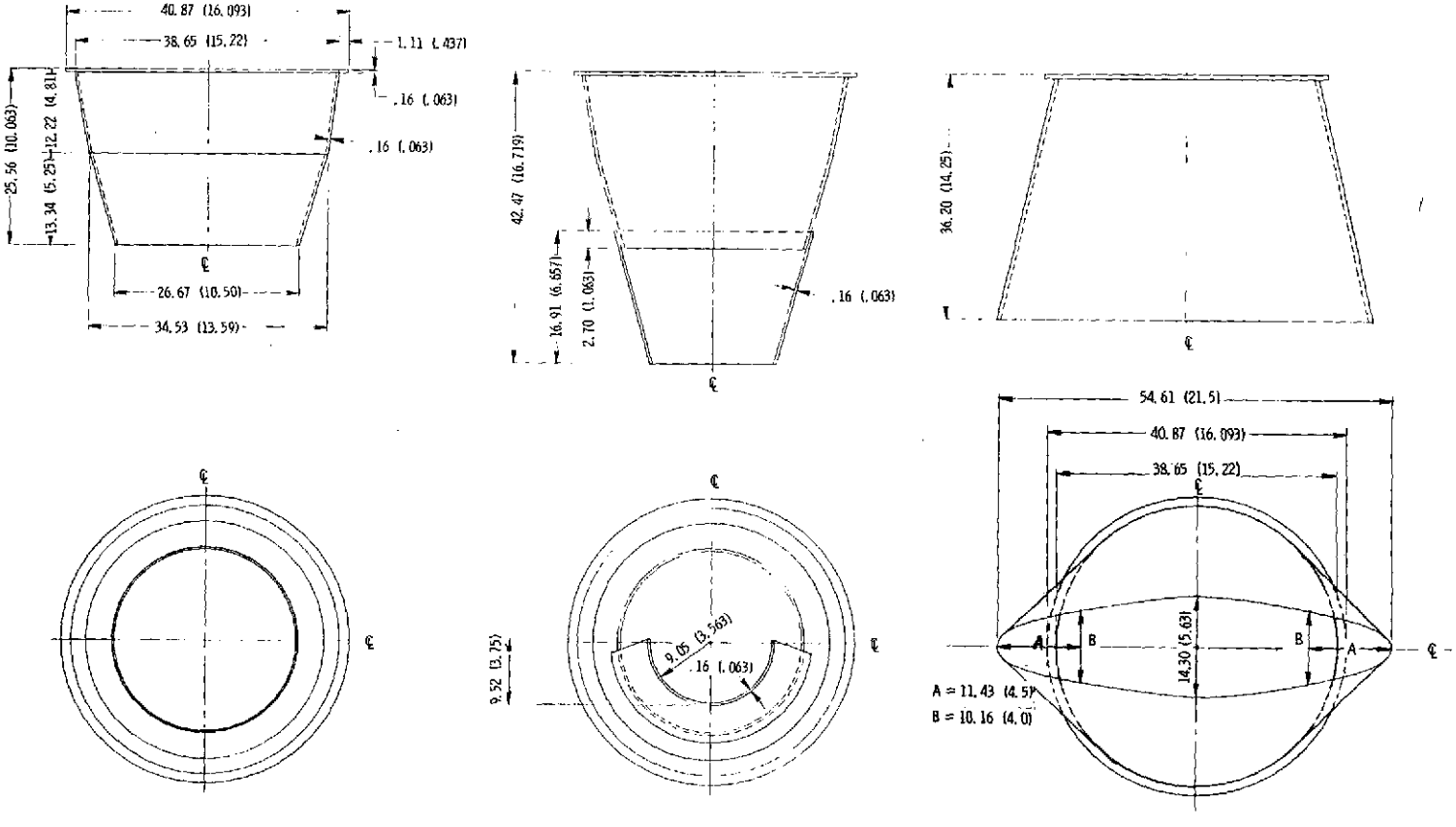

(a) Round nozzle. (b) Round nozzle with deflector. (c) Elliptical nozzle.

Figure 4.- Sketch of primary nozzles. Dimensions are in centimeters (inches).

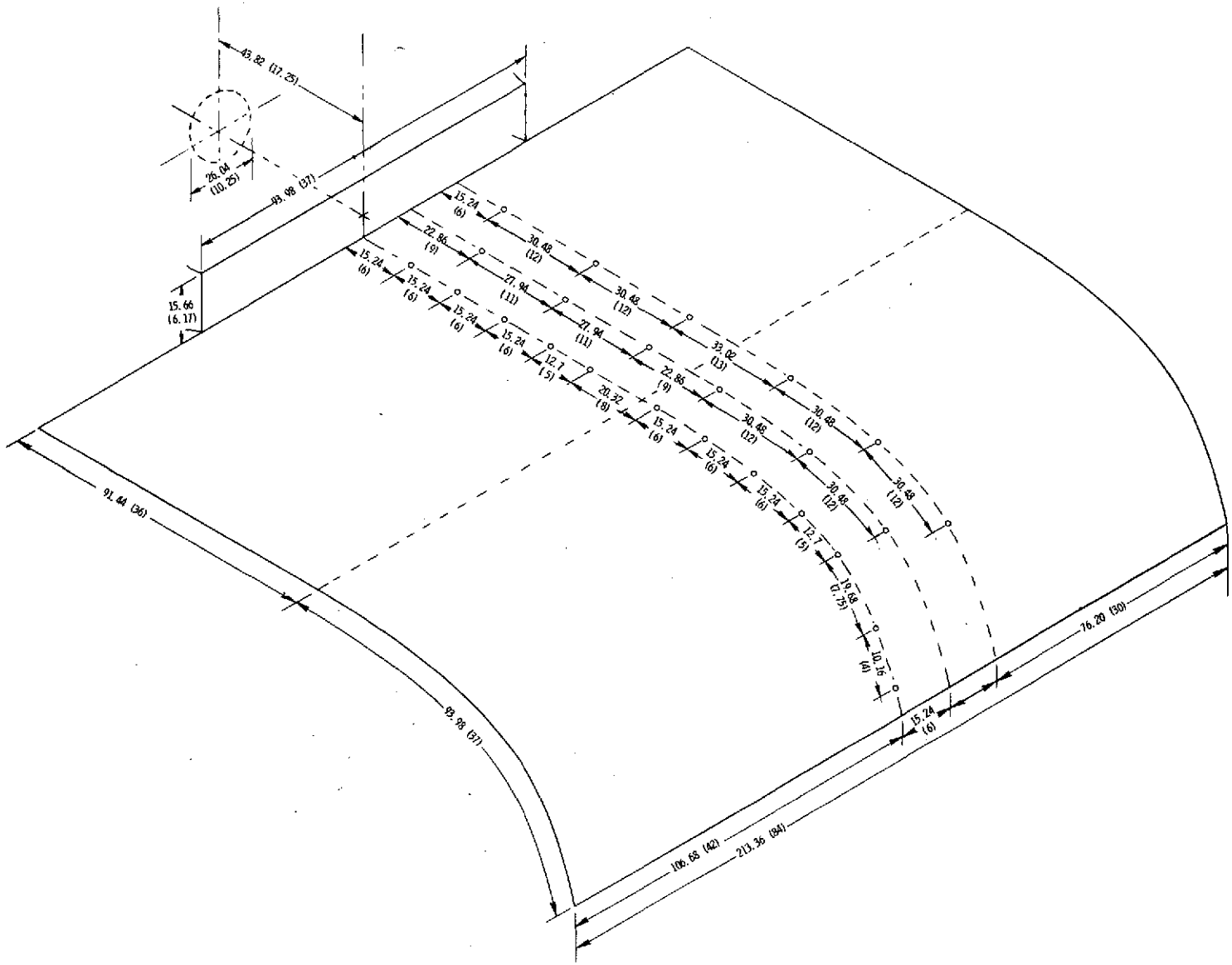

Figure 5.- Pressure-port locations on wing and flap. $\delta_f = 70^o$. Dimensions are in centimeters (inches).

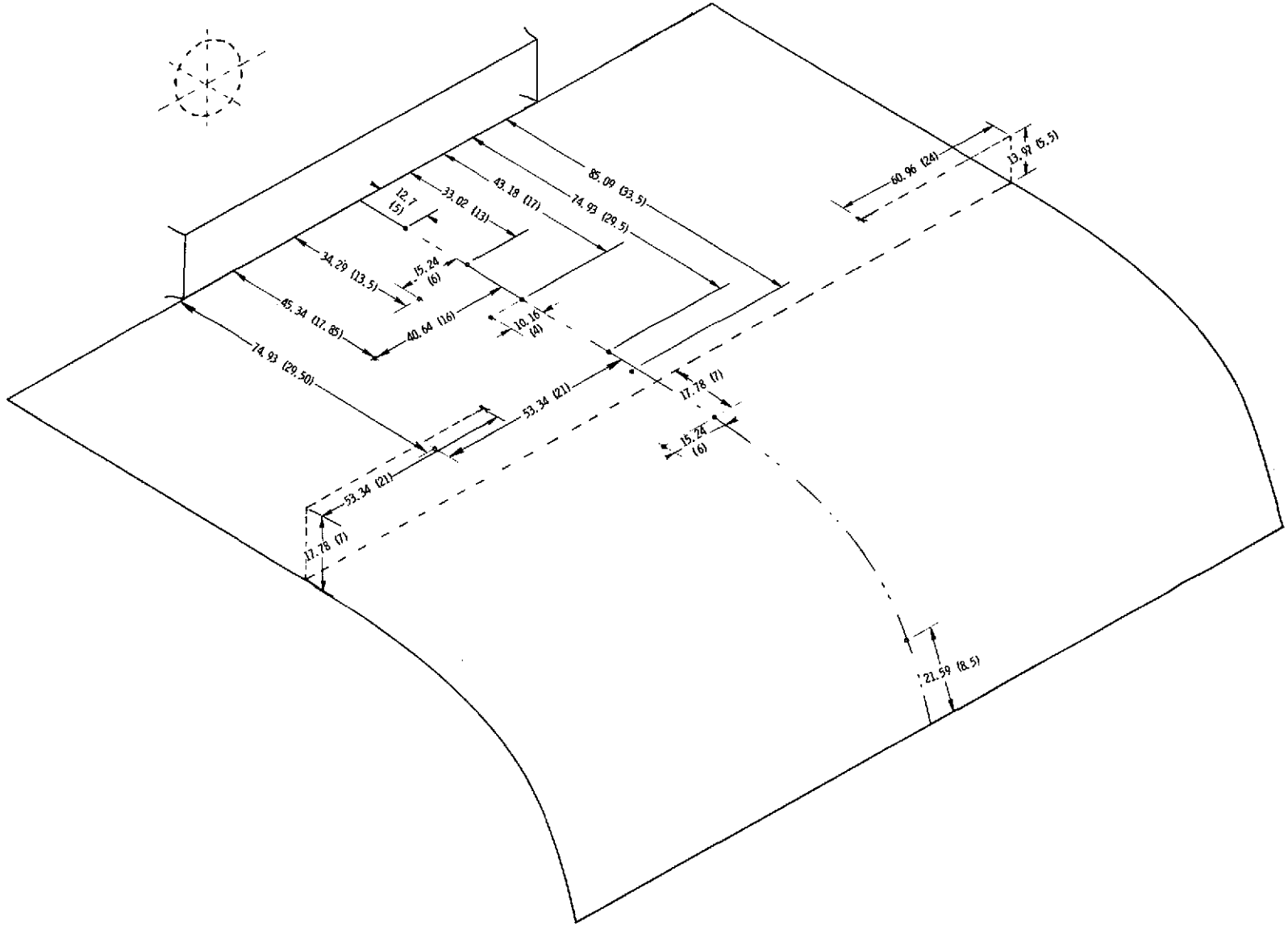

Figure 6.- Thermocouple locations on wing and flap. $\delta_f = 70^o$. All dimensions are in centimeters (inches).

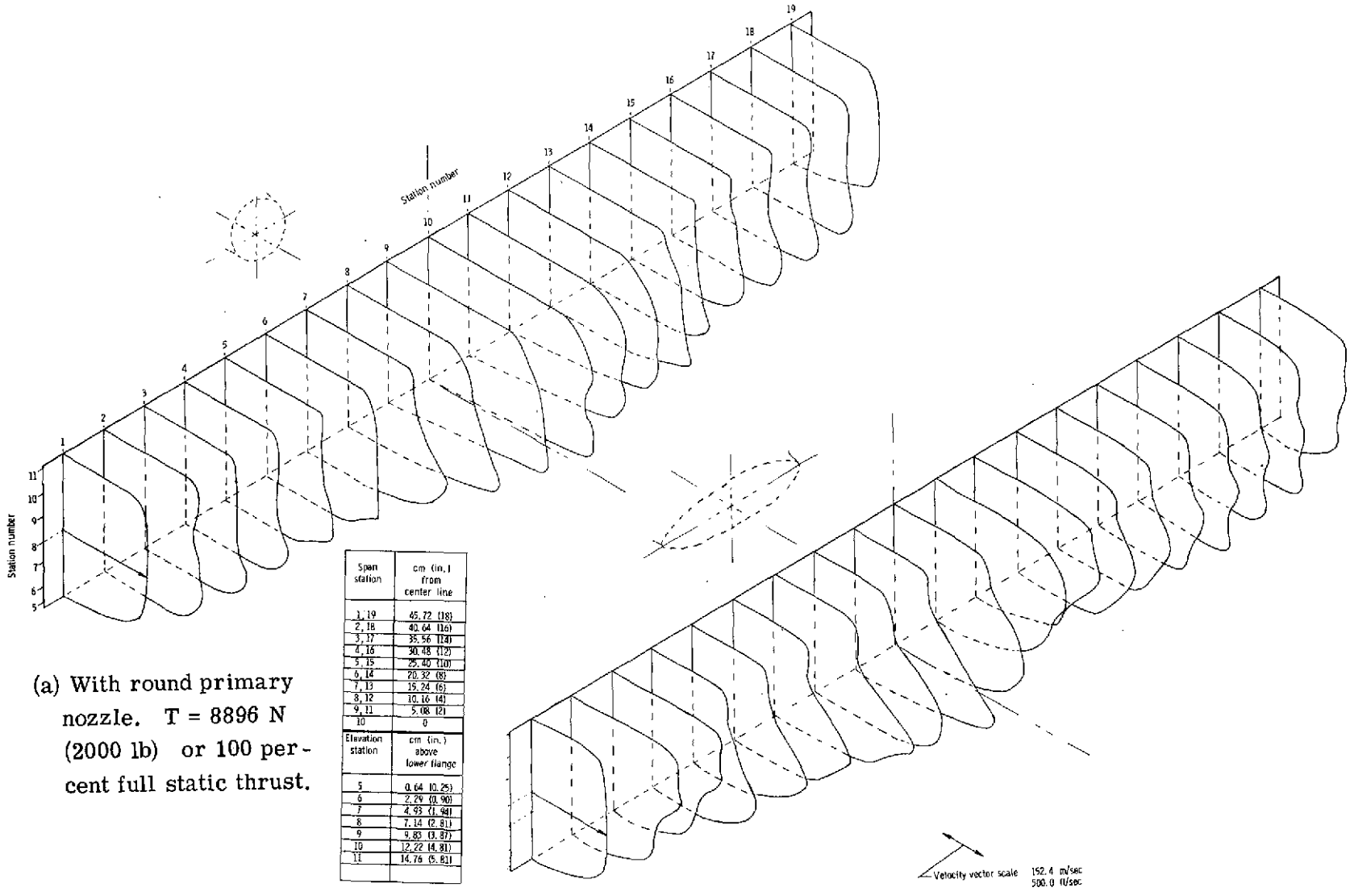

Span station	cm (in.) from center line
1, 19	45.72 (18)
2, 18	40.64 (16)
3, 17	35.56 (14)
4, 16	30.48 (12)
5, 15	25.40 (10)
6, 14	20.32 (8)
7, 13	15.24 (6)
8, 12	10.16 (4)
9, 11	5.08 (2)
10	0

Elevation station	cm (in.) above lower flange
5	0.64 (0.25)
6	2.29 (0.90)
7	4.93 (1.94)
8	7.14 (2.81)
9	9.83 (3.87)
10	12.22 (4.81)
11	14.76 (5.81)

(a) With round primary nozzle. T = 8896 N (2000 lb) or 100 percent full static thrust.

(b) With elliptical primary nozzle. T = 7784 N (1750 lb) or 87.5 percent full static thrust.

Figure 7.- Velocity profiles across the secondary exhaust nozzle.

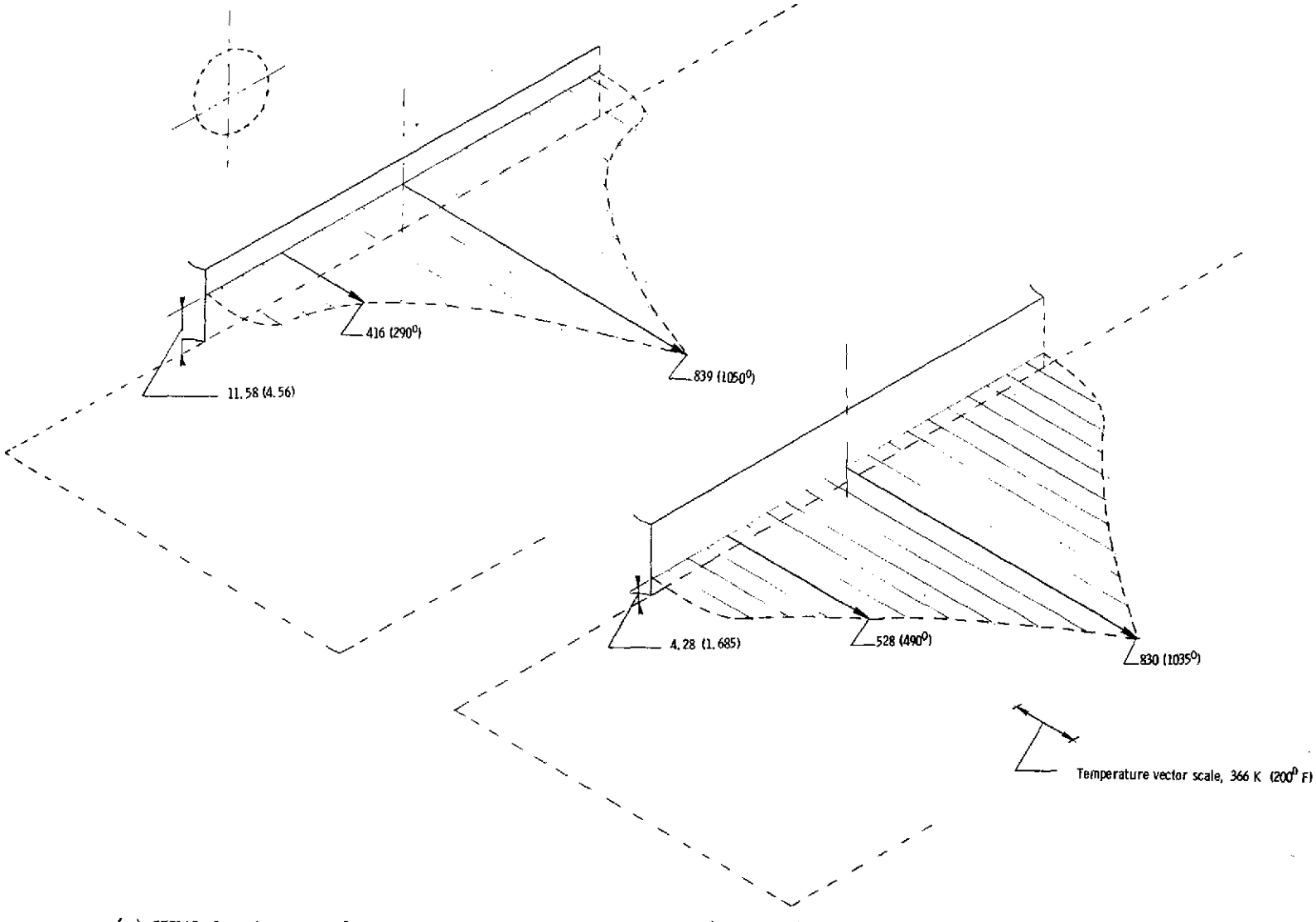

(a) With basic round primary nozzle. T = 8896 N (2000 lb) or 100 percent full static thrust.

Figure 8.- Temperature profiles of exhaust-gas efflux across the exit of the secondary nozzle. Linear dimensions are in centimeters (inches).

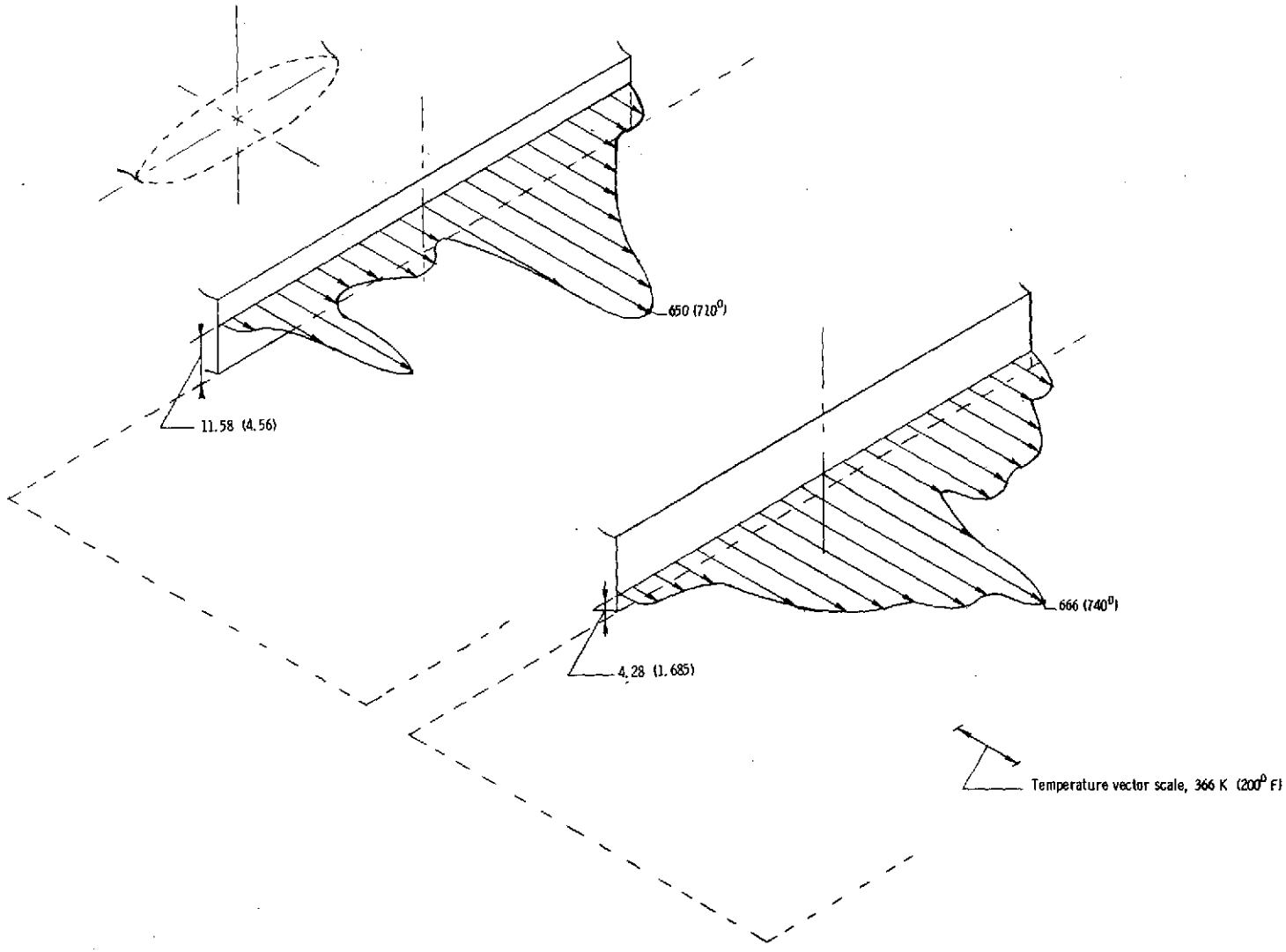

(b) With elliptical primary nozzle. T = 7784 N (1750 lb) or 87.5 percent full static thrust.

Figure 8.- Concluded.

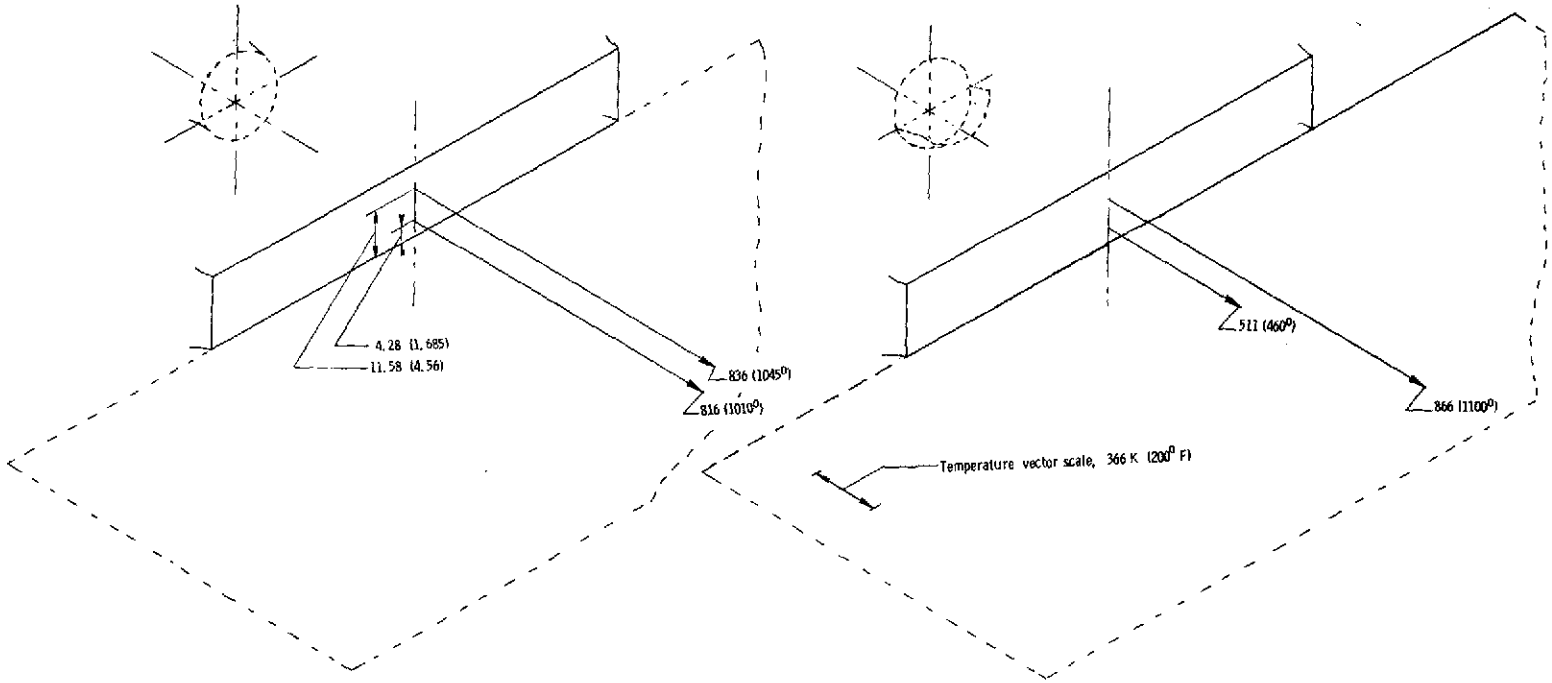

(a) With basic round primary nozzle.

(b) With deflector on round primary nozzle.

Figure 9.- Temperatures of exhaust-gas efflux at exhaust-exit center line. T = 8896 N (2000 lb) or 100 percent full static thrust. Linear dimensions are in centimeters (inches).

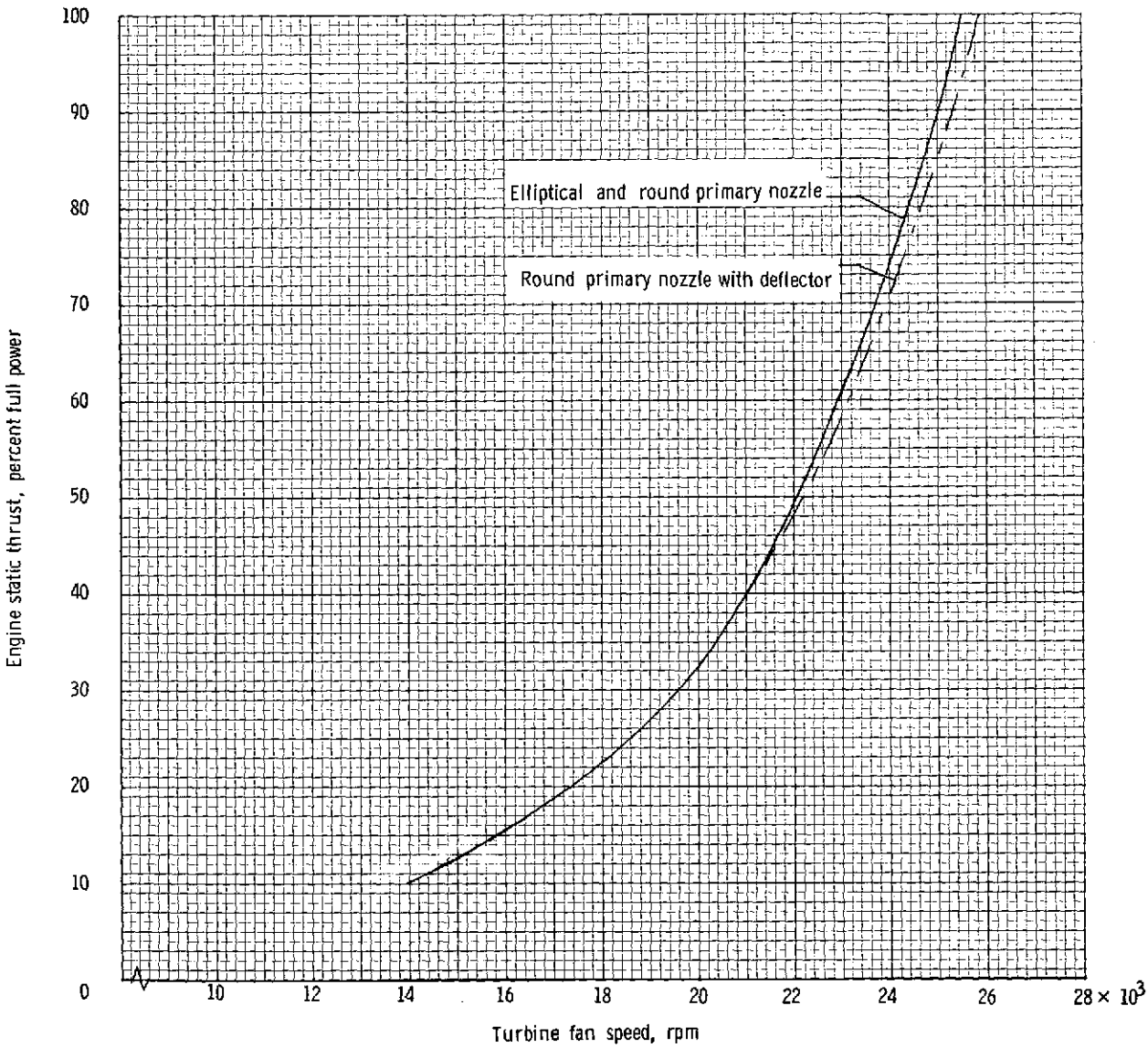

Figure 10.- Effect of primary-nozzle configuration on engine thrust for relatively constant ambient conditions. Temperature range of 275 K (35° F) to 277 K (40° F); 100 percent thrust referenced to 8896 N (2000 lb); bellmouth inlet.

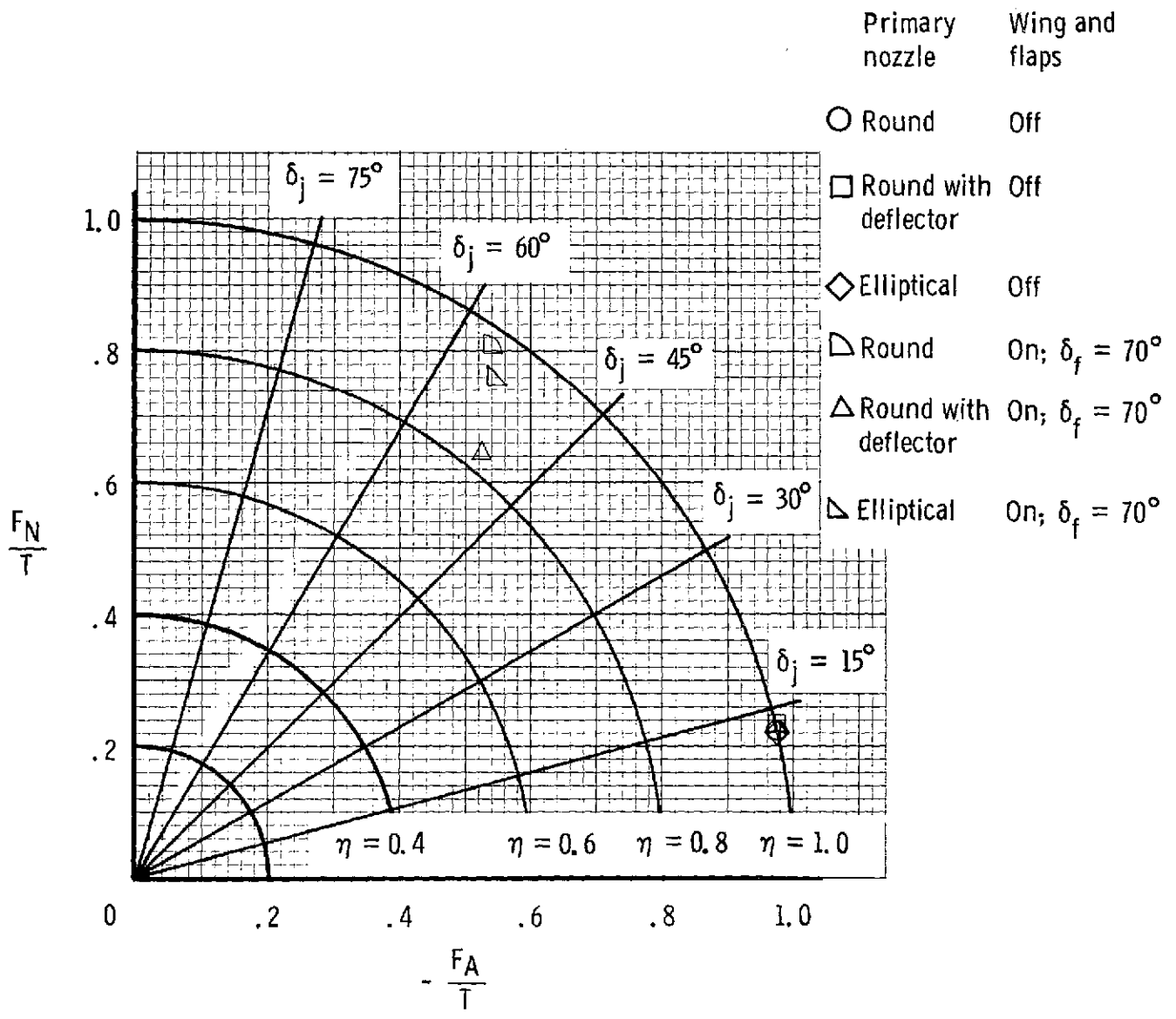

(a) Effect of primary-nozzle modifications. 100 percent full static thrust.

Figure 11.- Static turning performance.

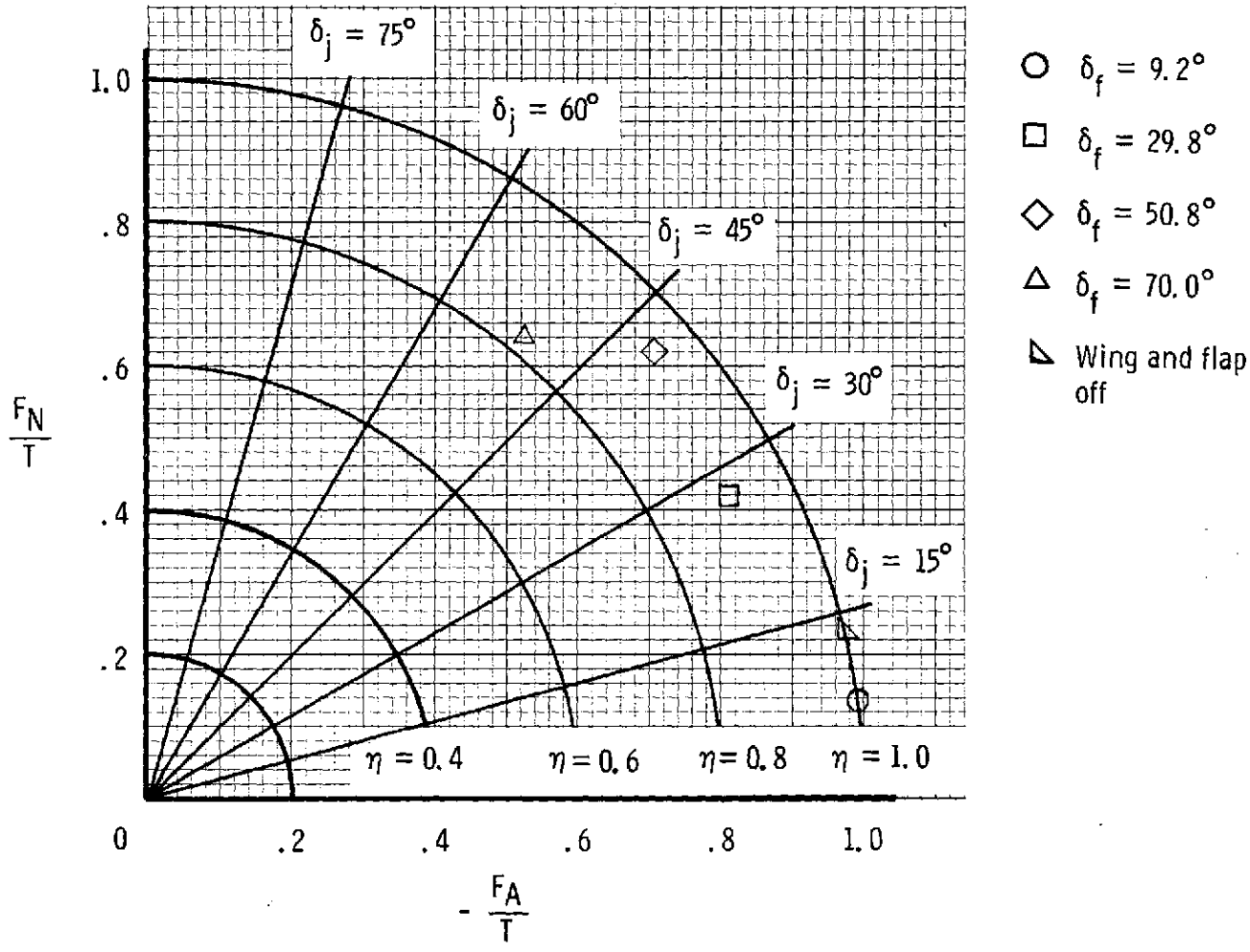

(b) Effect of flap deflection. Round primary nozzle with deflector.

Figure 11.- Continued.

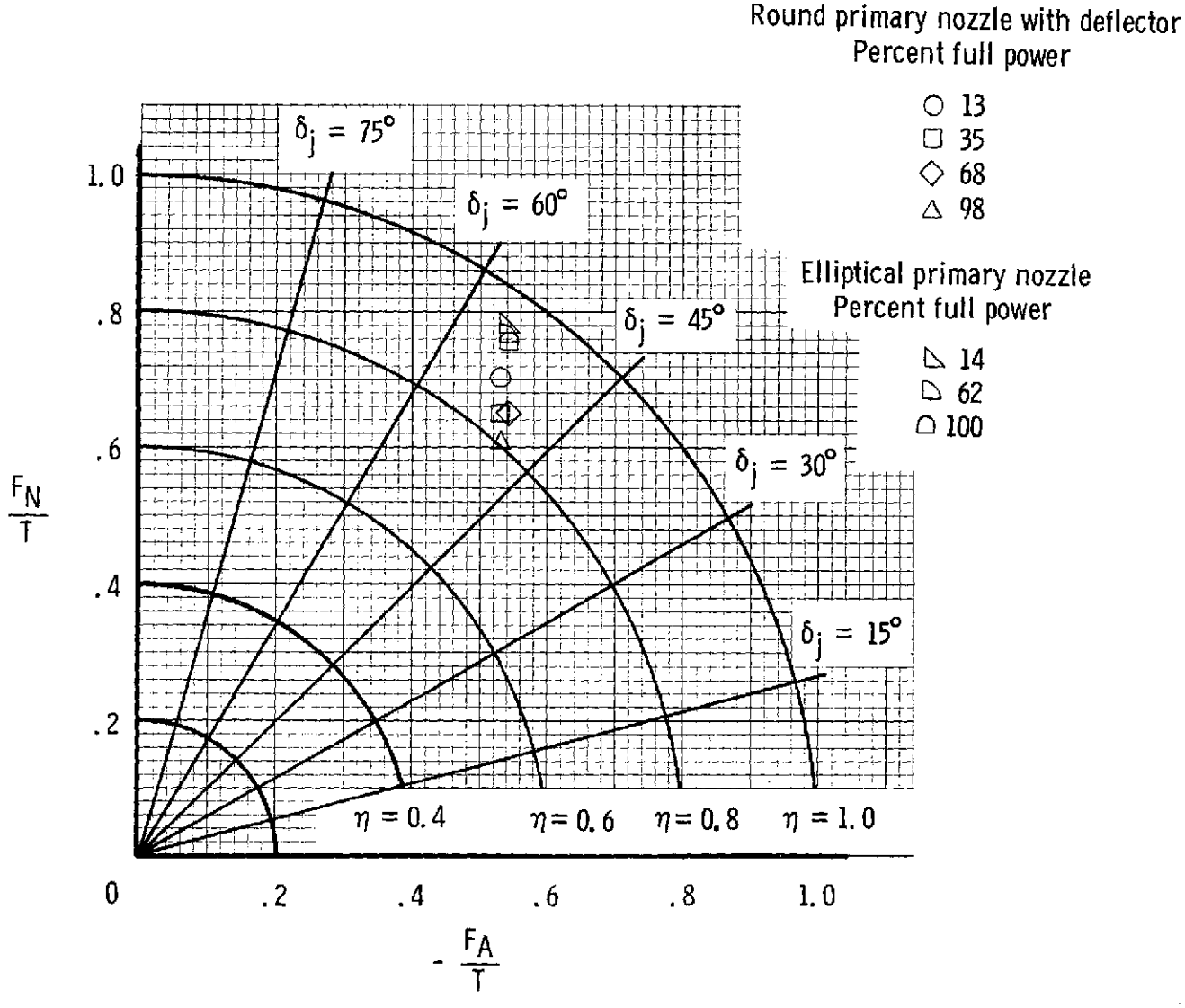

(c) Effect of thrust. $\delta_f = 70°$.

Figure 11.- Concluded.

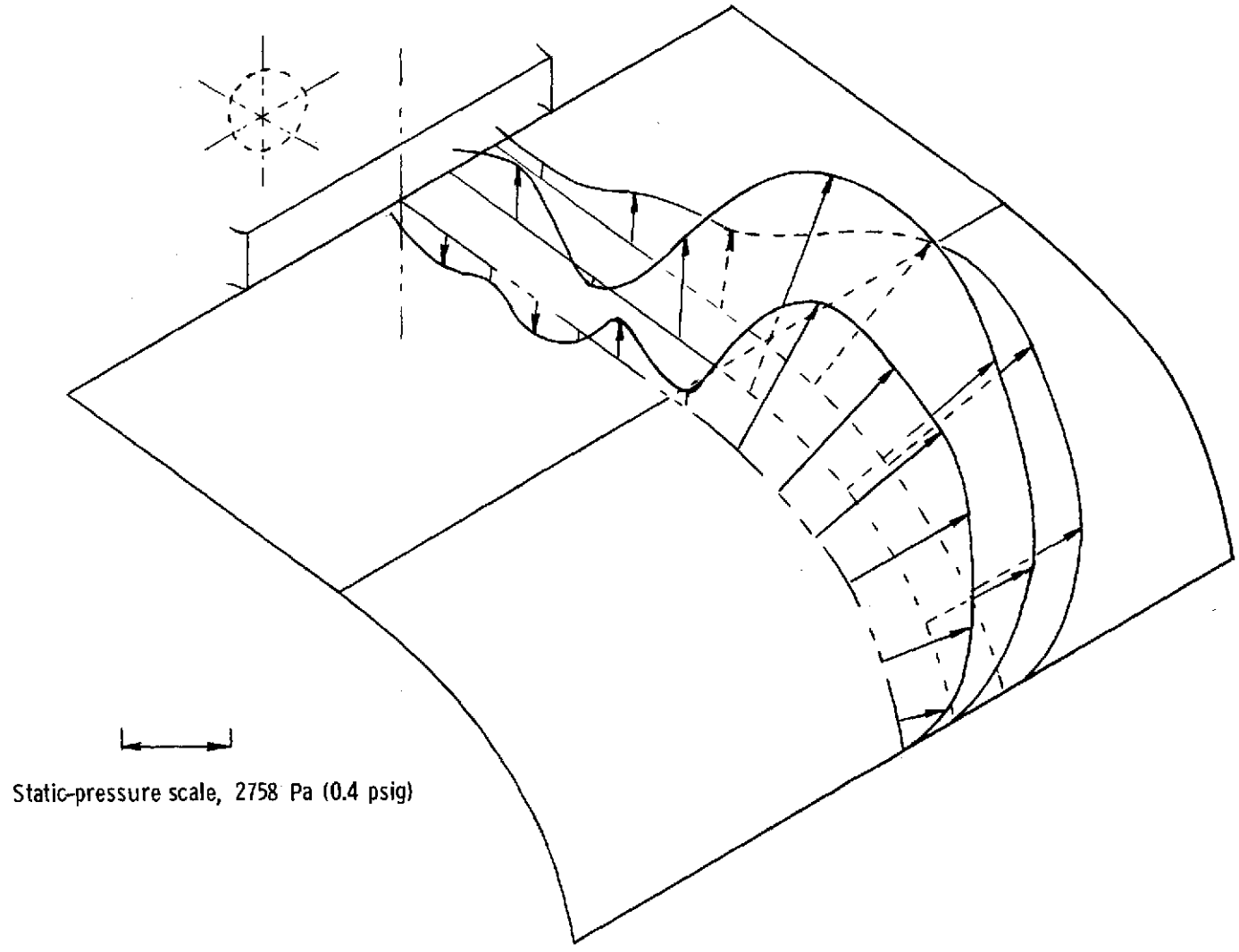

Figure 12.- Pressure distributions over wing and flap with basic round primary nozzle. 100 percent full static thrust; $\delta_f = 70^o$.

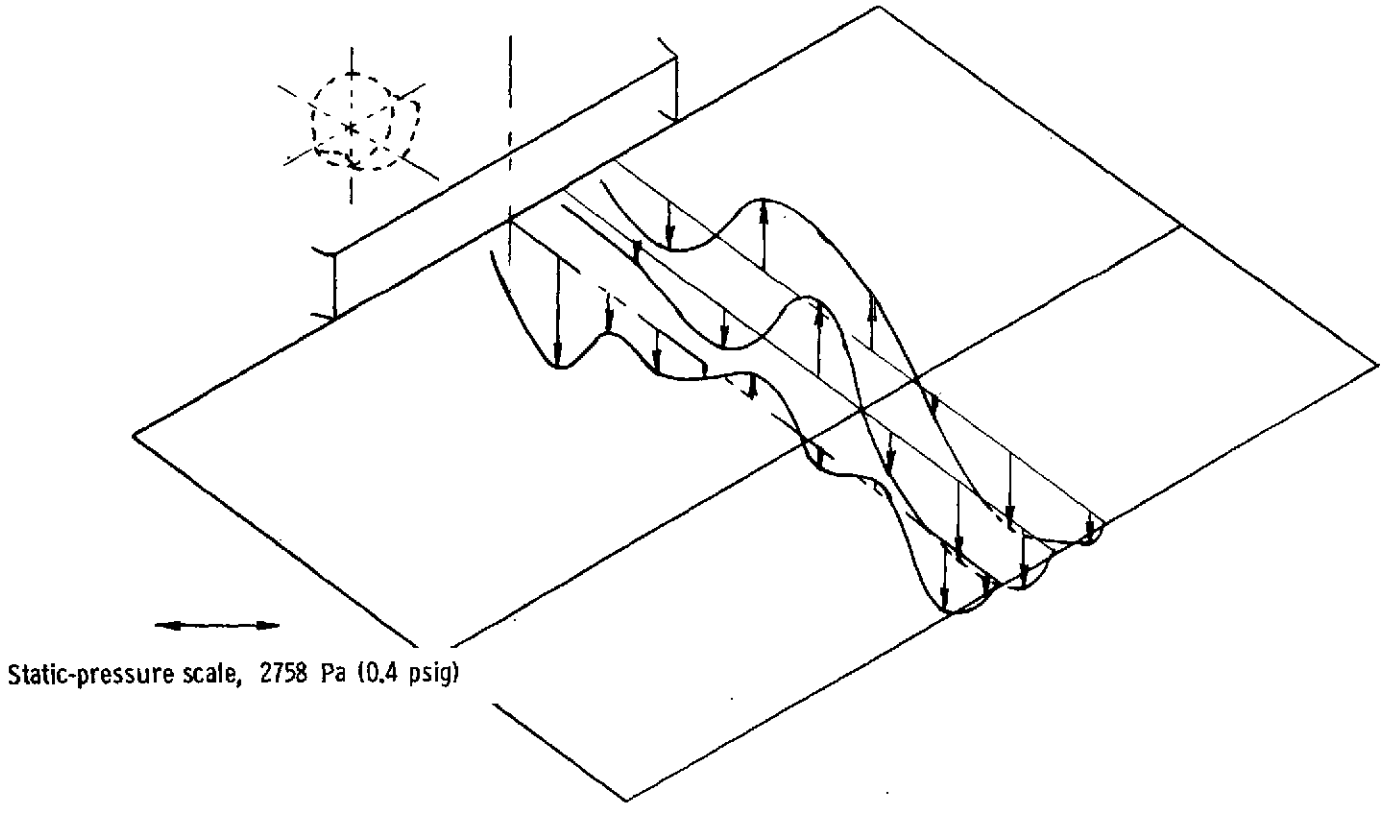

(a) $\delta_f = 9.2^o$.

Figure 13.- Pressure distributions over wing and flap with round primary nozzle with deflector. 96 percent full static thrust.

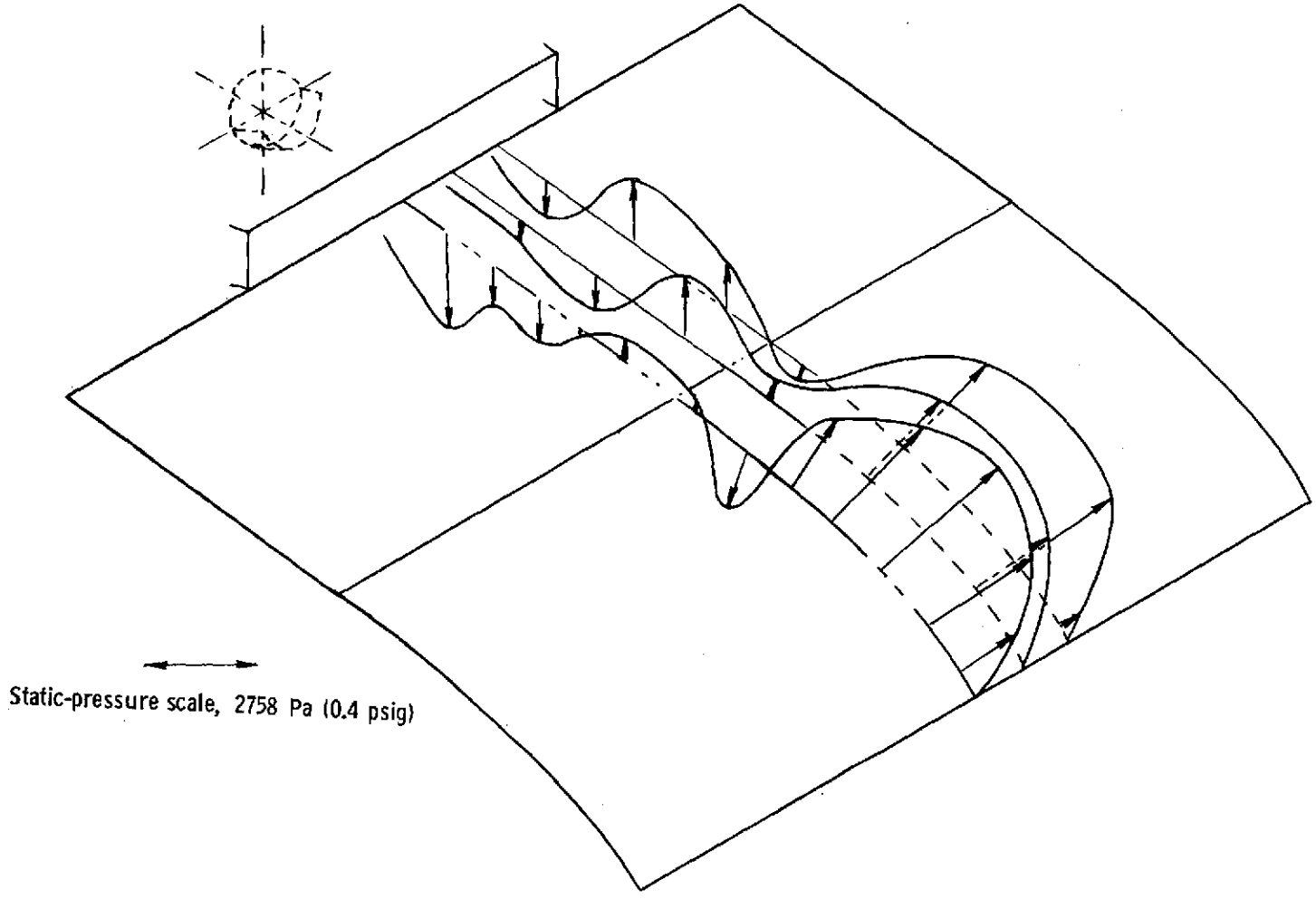

(b) $\delta_f = 29.8^o$.

Figure 13.- Continued.

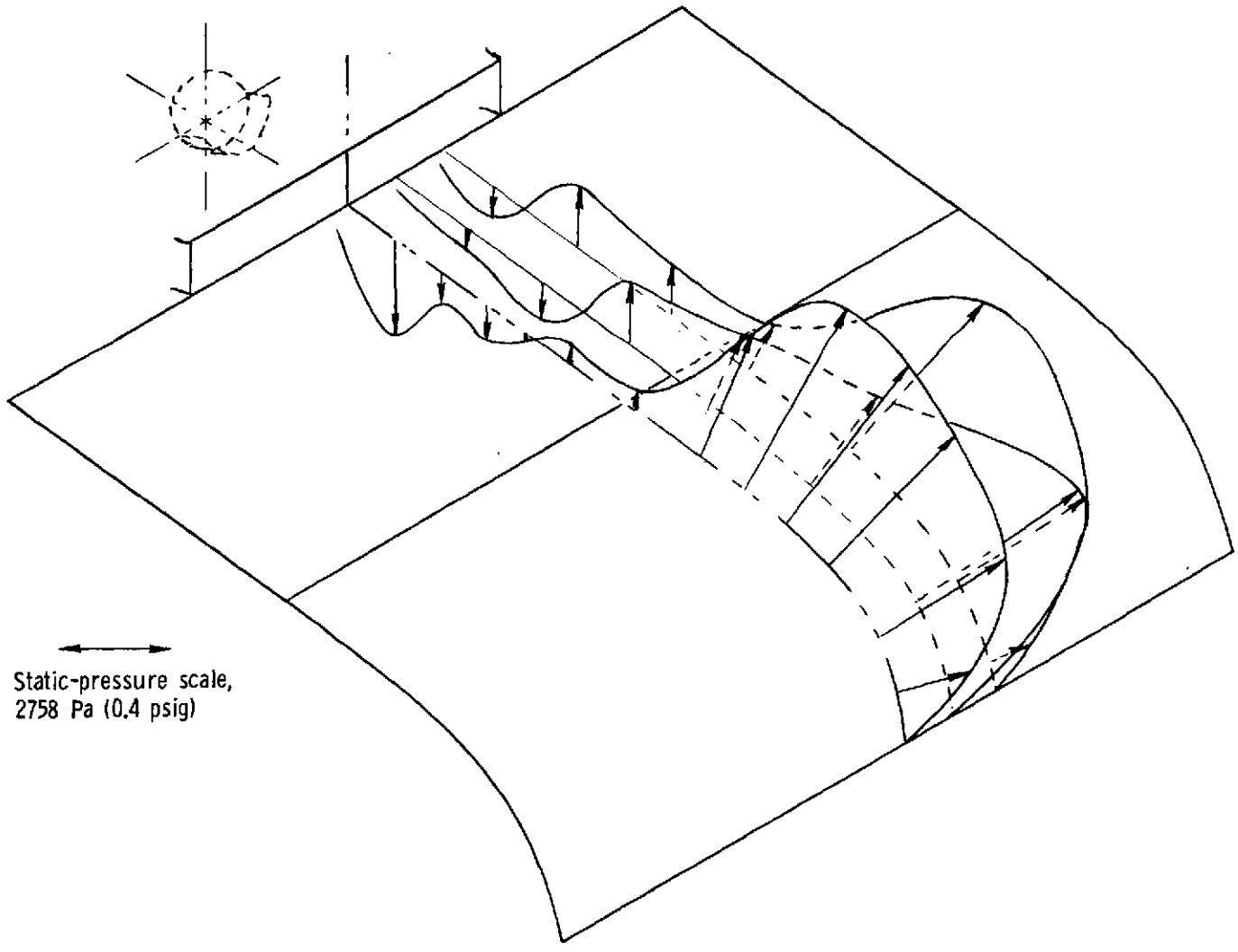

(c) $\delta_f = 50.8^o$.

Figure 13.- Continued.

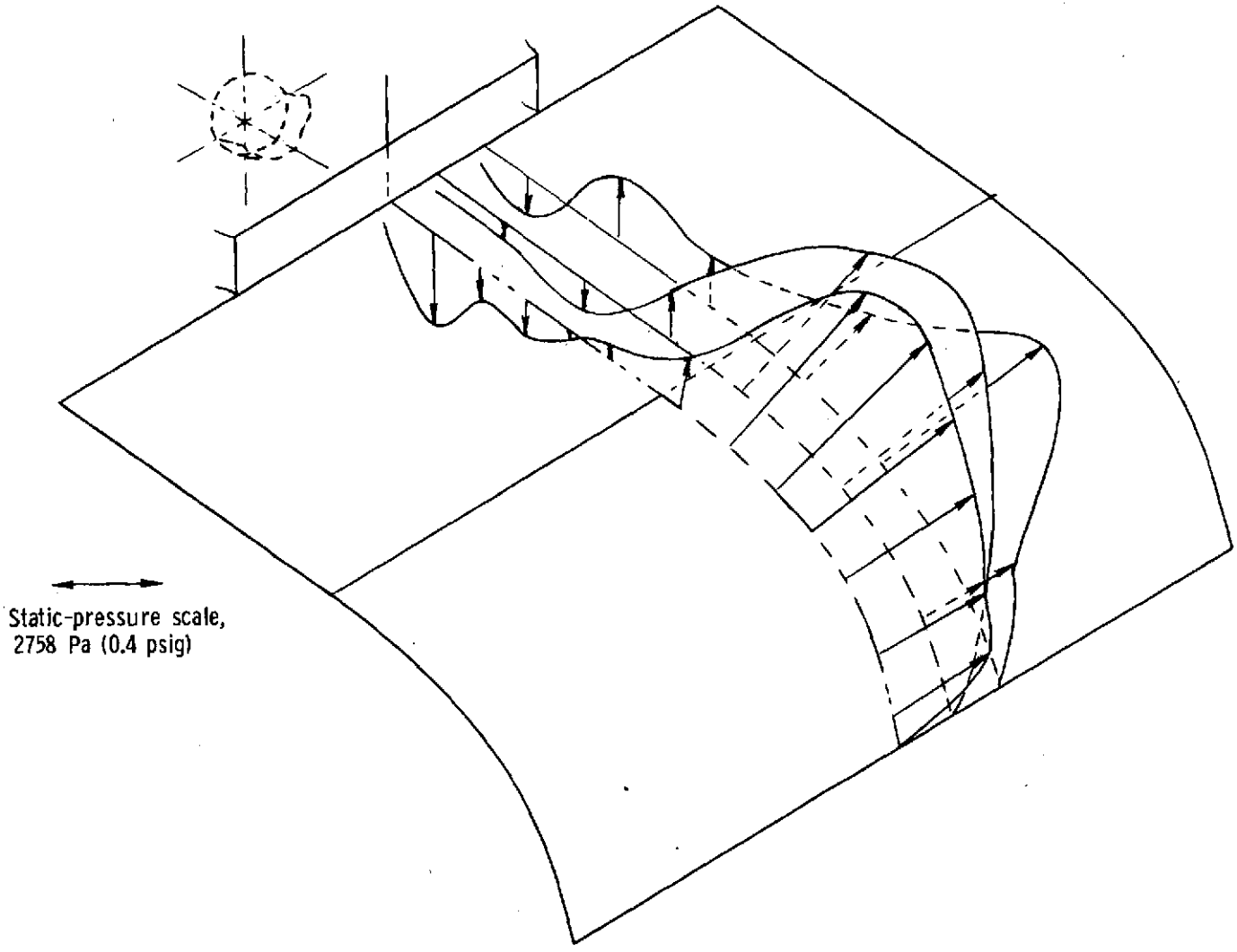

(d) $\delta_f = 70^o$.

Figure 13.- Concluded.

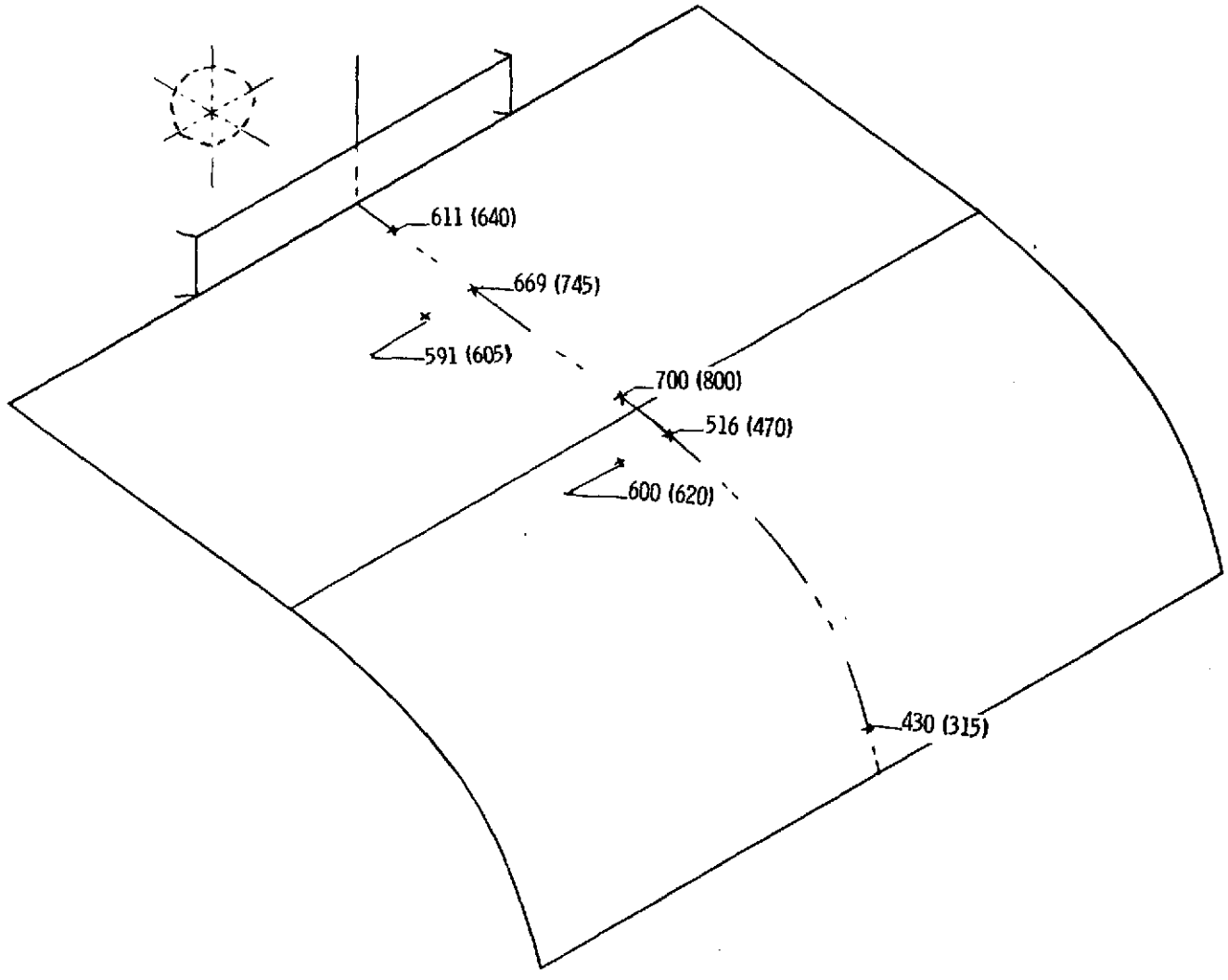

Figure 14.- Surface temperatures over wing and flap with basic round primary nozzle. 96 percent full static thrust; $\delta_f = 70^o$. Temperatures are in K (^oF).

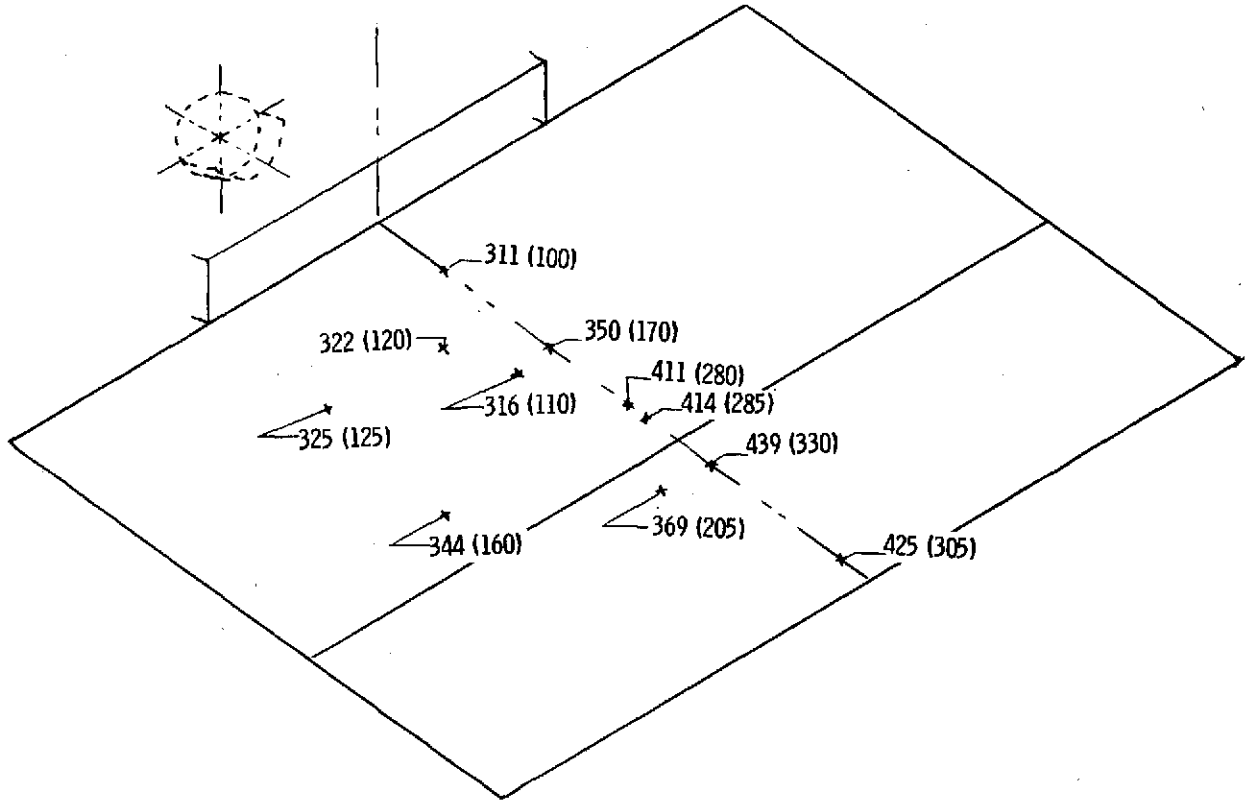

(a) $\delta_f = 9.2^o$.

Figure 15.- Surface temperatures over wing and flap with round primary nozzle with deflector. 96 percent full static thrust. Temperatures are in K (^{o}F).

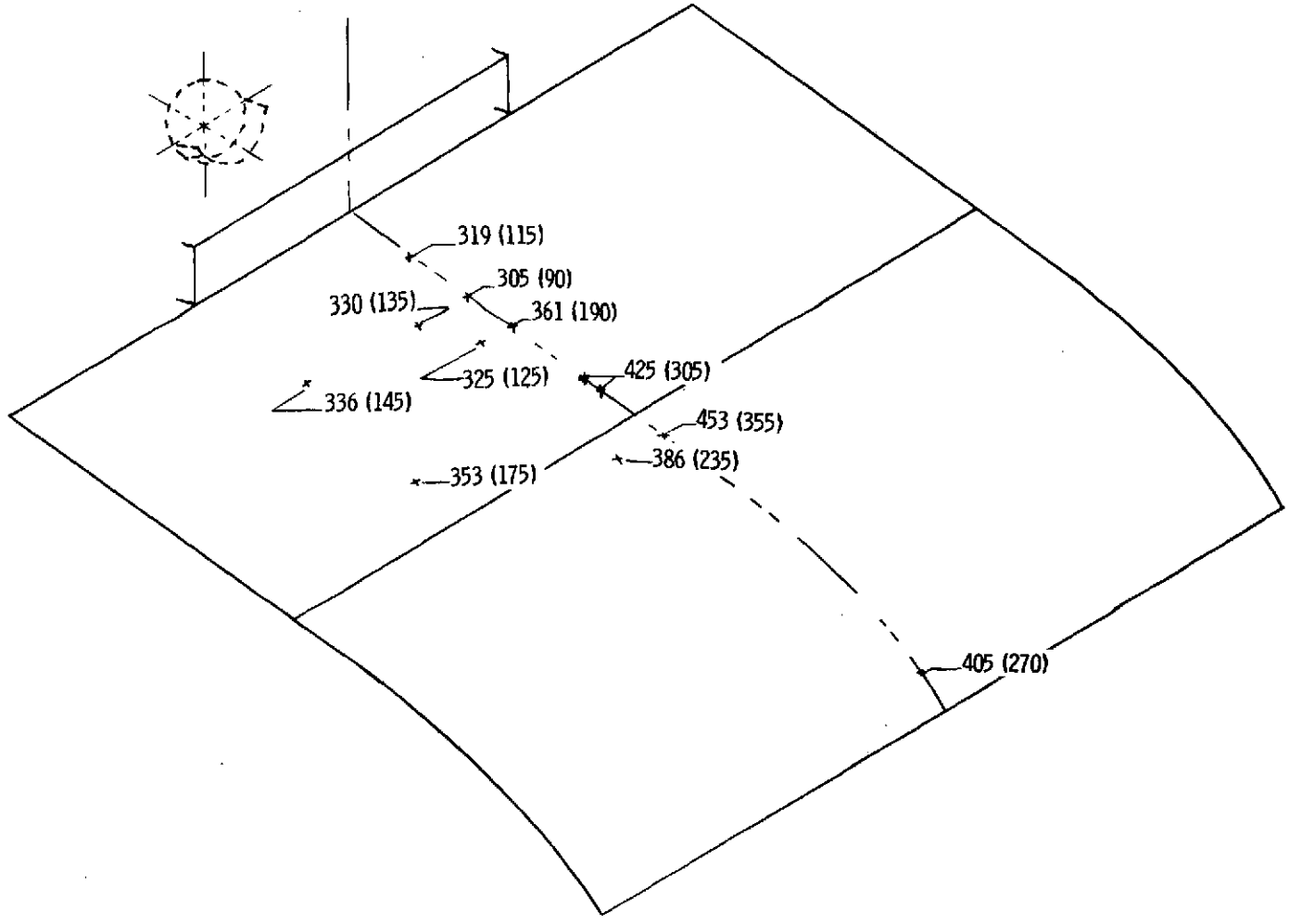

(b) $\delta_f = 29.8^o$.

Figure 15.- Continued.

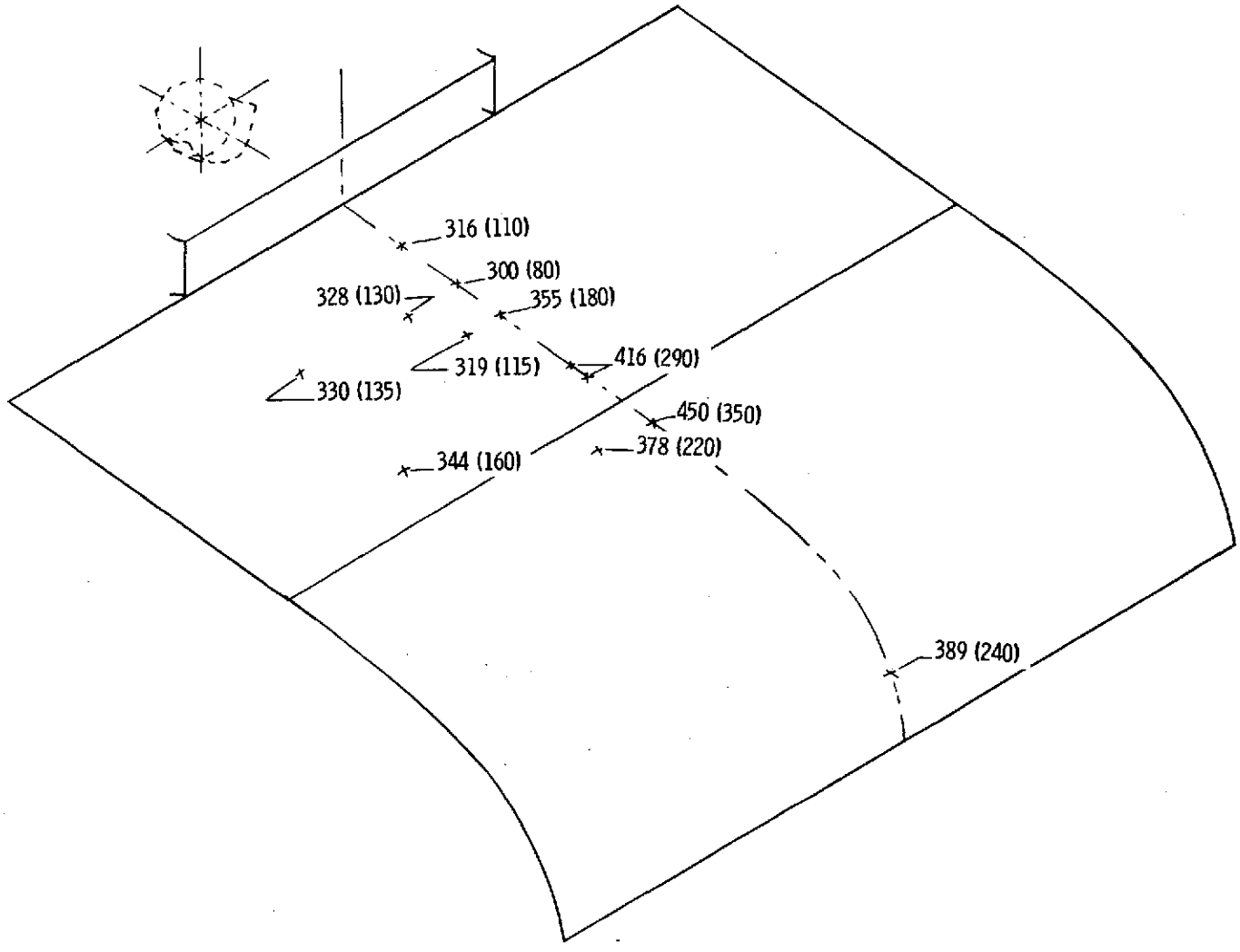

(c) $\delta_f = 50.8^\circ$.

Figure 15.- Continued.

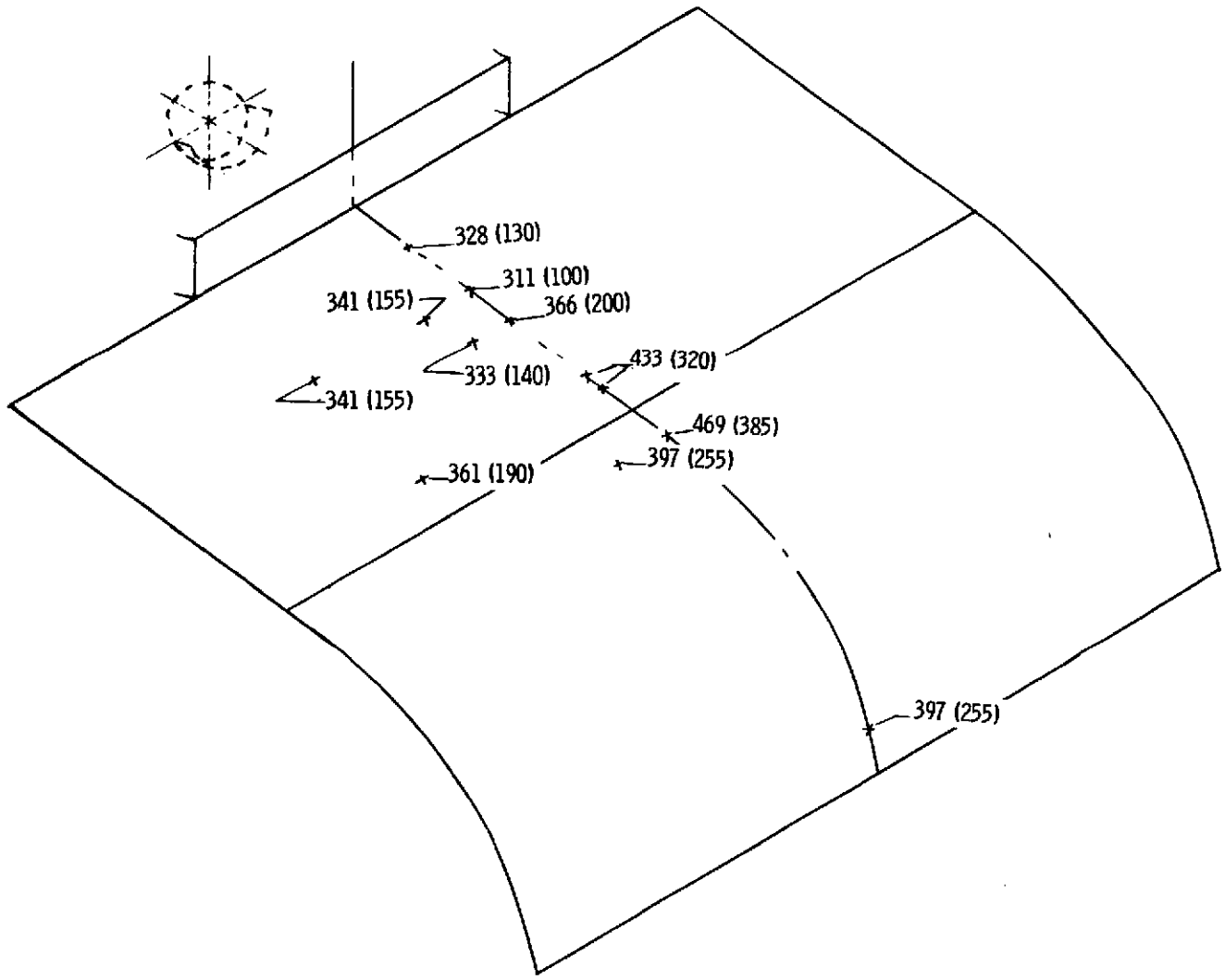

(d) $\delta_f = 70^o$.

Figure 15.- Concluded.

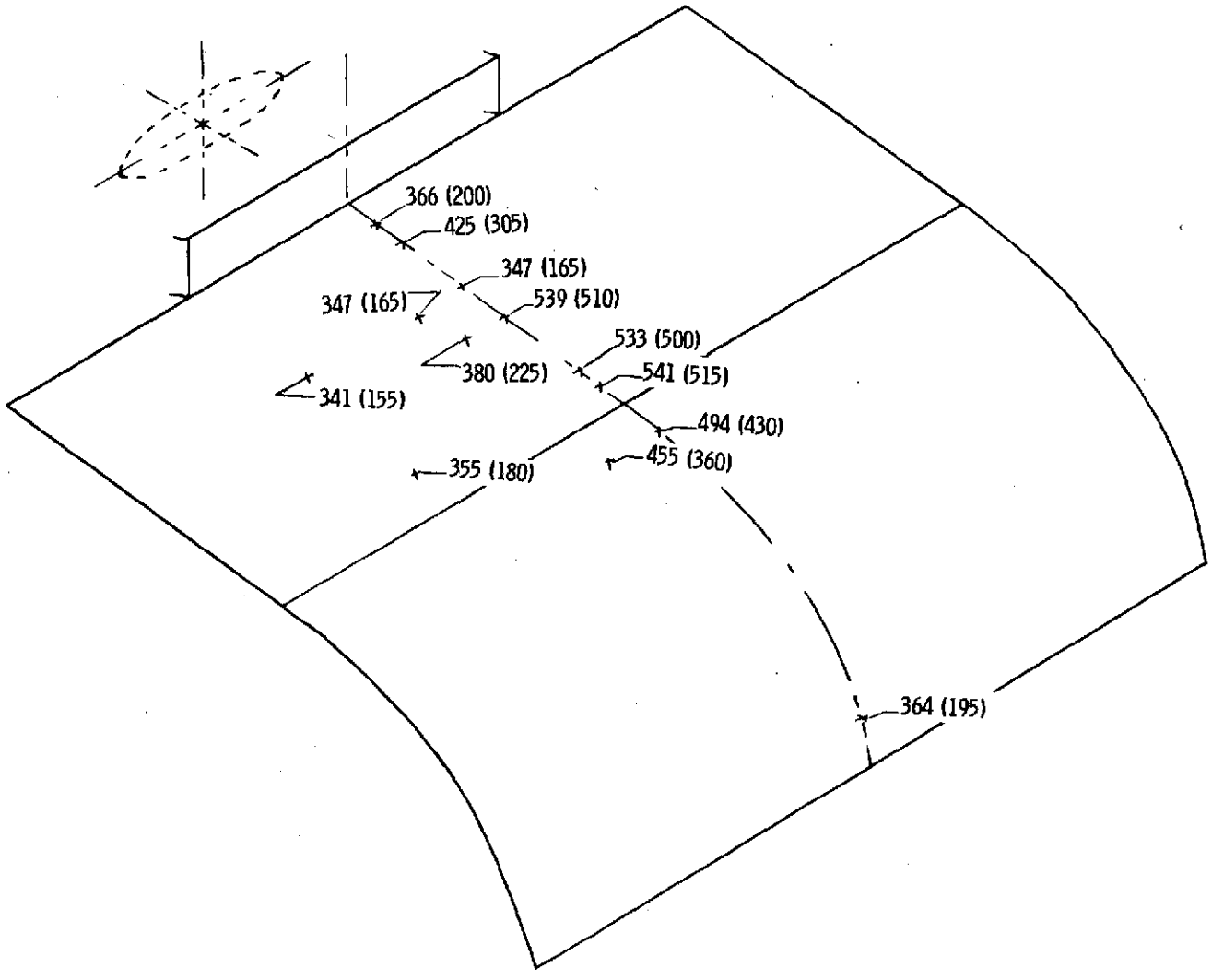

Figure 16.- Surface temperatures over wing and flap with elliptical primary nozzle. 96 percent full static thrust; $\delta_f = 70^o$. Temperatures are in K (^{o}F).

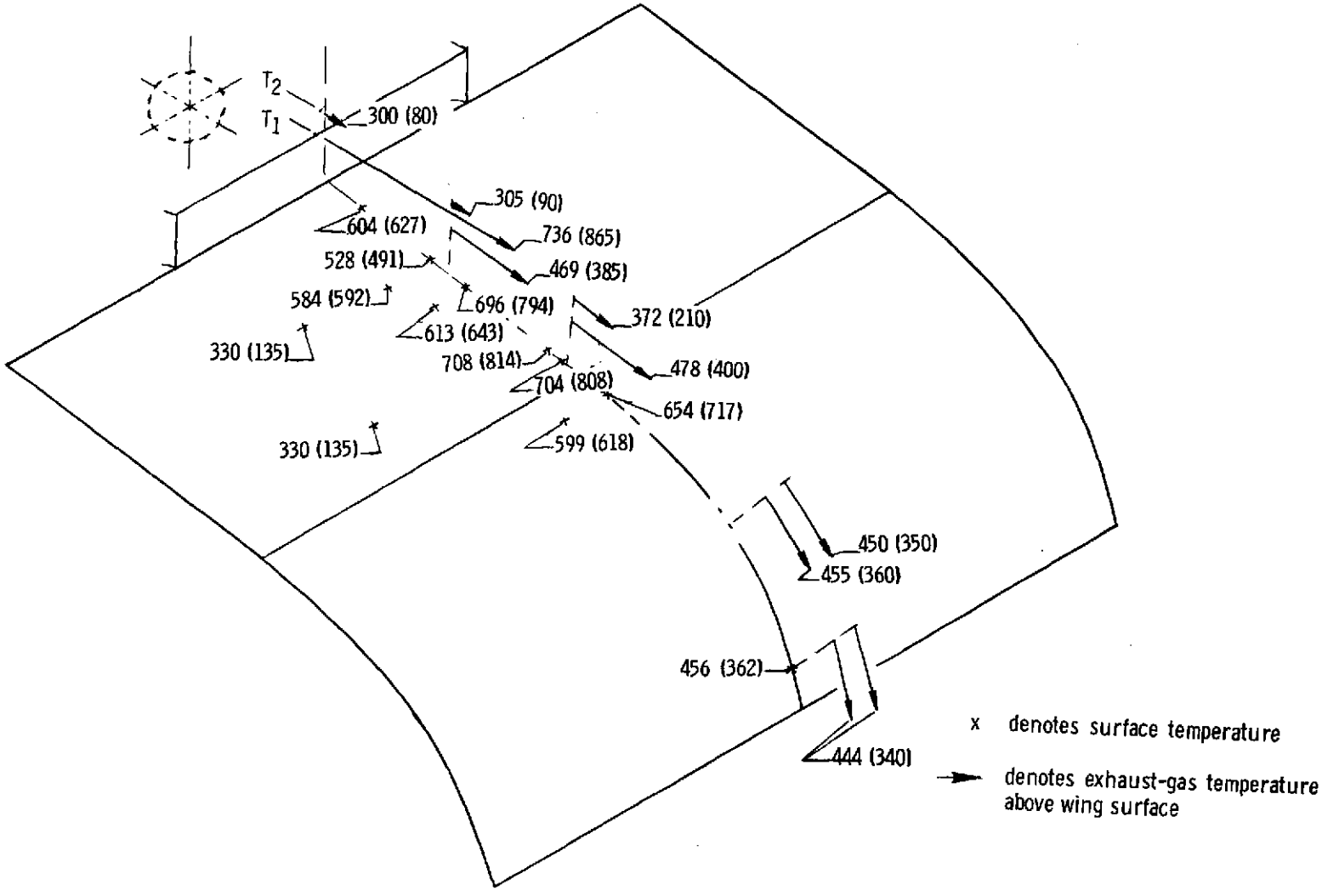

Figure 17.- Temperatures of exhaust-gas efflux on exhaust-exit center line at five chordwise stations. Surface temperatures averaged for five runs; basic round primary nozzle; $\delta_f = 70^o$; 96 percent full static thrust; T_1 and T_2 measured 13.02 cm (5.125 in.) and 20.32 cm (8.00 in.) above surface, respectively. Temperatures are in K (^oF).

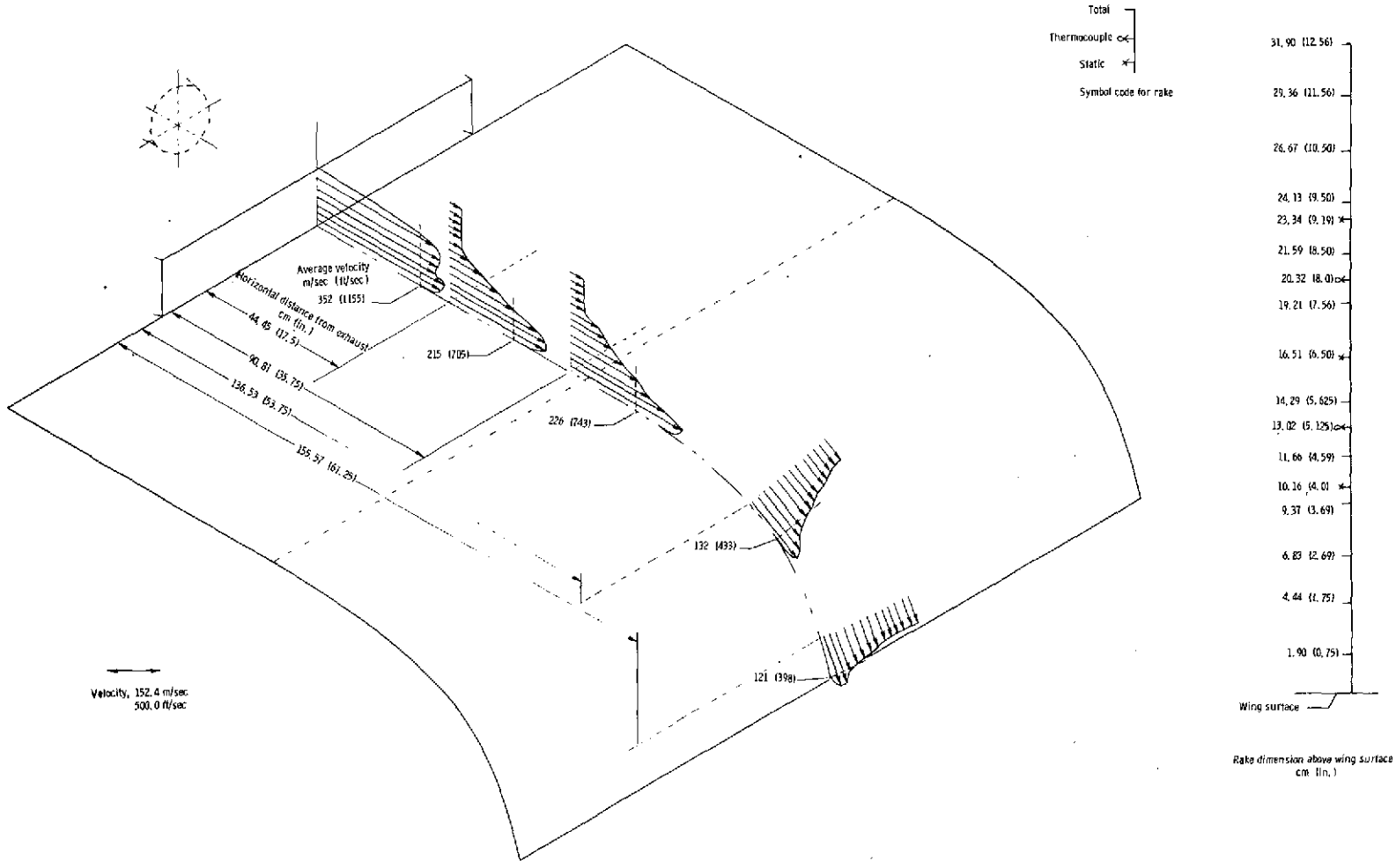

Figure 18.- Velocity profiles above the wing and flap at five chordwise stations. Basic round primary nozzle; $\delta_f = 70^o$; 96 percent full static thrust.